# FLUID MUD FORMATION

by Leo van Rijn; www.leovanrijn-sediment.com

## 1. Fluid mud definitions

Fluid mud is a high-concentration suspension of fine sediment particles (< 63 μm) in which settling is substantially hindered by the close proximity of sediment particles and flocs, but which has not formed an interconnected matrix of bonds (gelling concentration) strong enough to eliminate the potential for mobility, see overview of McAnally et al. 2007. Flocculation/aggregation of the primary fine sediment particles into larger, multiple-particles, or flocs, occurs before and during the hindered settling phase. Fluid mud can be present as an intermediate stage before consolidation. Fluid mud consolidates to form a bed layer with dewatering and sinking of the bed surface (in the absence of sediment supply from above). Consolidation can continue for days to years.

The formation of fluid is strongly related to the percentage of clay particles < 4 μm and the percentage of organic materials (organic-rich sediments). The formation of fluid mud is highly promoted if the clay fraction is larger than 50%. Organic-rich fluid muds are characteristic of shallow eutrophic lakes. Where fluid mud is persistent in relatively quiescent environments such as lakes, large amounts of organic matter can play a role in inhibiting dewatering and maintaining the fluid state of the bed. Organic-rich fluid muds found in subaqueous deltas and estuaries and along high-energy coasts tend to contain less organic matter (<5%). High organic matter and contaminant accumulation are more likely to be a problem in low energy (stagnant) fluid muds.
The clay fraction consists of platey, cohesive minerals from the class of clays and micas, with the specific minerals depending on the local conditions: chlorite, illite, smectite, montmorillonite and kaolinite.

Fluid mud generally has viscoplastic (pseudoplastic) properties which means that a finite yield stress can be defined below which the relationship between shear stress and shear rate is linear (Newtonian behaviour) and above which there is non-linear behaviour with permanent deformation of the matrix structure. The rheological behaviour can be tested in roto-viscometers. The rheological properties of fluid mud (viscosity, yield stress, flow point stress) are dependent on its stress history. Fluid mud viscosity and yield stress decrease with time when subjected to a constant, sufficiently high strain or stress. This thixotropic decrease in strength is gradually regained after a certain quiescent resting period.

Fluid mud forms in river, lake, estuarine, and shelf environments when the amount of fine sediment entering the near-bed layer is greater than the dewatering rate of the high-density suspension. This may occur due to convergent horizontal advection of sediment-laden flow and/or may be the result of settling from above during periods of decelerating or slack currents.

Fluid mud layers can be formed by the following processes:

- deposition of fines as mobile fluid mud in tidal channels during periods with low flows (decelerating and slack tides; neap tides); fluid mud formed during periods of decelerating and slack tide conditions will normally re-entrained by the accelerating currents after slack water except during neap tides;
- deposition of fines as stagnant fluid mud in dredged channels and mooring/turning basins due to reduction of the flow velocity in larger water depths (as thick layers of fluid mud depending on dredging regime);
- deposition of fines as mobile fluid mud at coastal shelfs (depths of 10 to 20 m) in the surrounding of nearby tidal inlets (fluvial sources) in conditions with relatively low swell waves (< 2m) and episodic storm wave events;

- fluidisation of the top layers of consolidated mud beds due to the presence of wind waves and ship waves (Van Rijn 1993); waves can loosen a cohesive sediment bed and generate fluid mud; the soil matrix is destroyed by excess pore pressure buildup and an upward moving pore fluid is generated which exerts a drag force on the sediment aggregates that exceeds the effective weight of the particles and/or the strength of higher order inter-aggregate bonds; the fluid mud quickly reconsolidates into a fairly firm bed when waves stop.

Fluid mud can flow down bottom slopes (typical critical slopes are $1^o$ to $2^o$) as a gravity/density/turbidity current or horizontally as streaming due to overlying currents and waves. Density currents refer to currents that are kept in motion by the force of gravity due to small differences in density. Turbidity currents denote density currents for which excess density is produced by the presence of suspended solids in strong interaction with the mobile sediment bed. Turbidity currents can be caused by catastrophic failures (seismic shocks or storm waves).

Management of sedimentation can be accomplished by various techniques,which are based on:

1. keep sediment out,
2. keep sediment moving, or
3. remove sediment once it has deposited.

This simple and useful classification can be adapted to fluid mud management techniques that accomplish: source control; formation control (including nautical depth definition) and removal.
The Rotterdam harbour authorities have defined a density criterion of 1200 kg/m$^3$ for navigable or nautical depth in 1974, which means that ship are manoeuvring through mud with wet bulk density of 1000 to 1200 kg/m$^3$. Mud shear strength and/or viscosity (based on rheological tests) can serve as the basis for navigable depth criteria and definition of the bottom. Agitation techniques/dredging can alter the vertical suspension profile and have become known as active nautical depth procedures. In-situ conditioning by hopper pumping/dredging is a new approach, which employs agitation plus aeration to keep fluid mud density and/or viscosity above threshold values for navigability. Short exposure to air can lead to rapid re-oxygenation of the mud. The conditioned aerobic mud is then reinserted into the fluid mud cloud at its in-situ density.

## 2. Fluid mud concentrations

### 2.1 Layer schematization

In muddy conditions with high tidal velocities (> 1 m/s), various high-concentration layers of mud may be present in the water column, which can be detected by acoustic sounders. These sounders emit an acoustic pulse that propagates through the fluid, returning reflections from the muddy materials. Multiple frequencies can be used to detect layers (interfaces/lutoclines) with different densities. The upper fluid mud surface can be detected using 210 kHz high-frequency, wheres the surface of more consolidated surface (subsoil) can be detected using 33 KHz low-frequency.
The mud concentrations (in the range of 1 to 100 kg/m$^3$) of the mud suspension can be measured using optical sensors (OBS). Acoustic sensors can be used to determine the fluid mud concentrations in the range of 100 to 1000 kg/m$^3$. Both sensors need many pump samples for calibration. Nuclear transmissance and backscatter techniques have both been demonstrated to measure the bed mud density accurately, but licensing and safety measures are required.

Generally, a three-layer system can be distinguished in vertical direction (see **Figure 2.1**), as follows:

- **Consolidated mud layer** at the bed surface with concentrations larger than about 200 to 300 kg/m³. The flocs and particles are supported by the internal floc framework.
- **Fluid mud suspension layer** with concentrations in the range of 10 to 300 kg/m³. The layer thickness is of the order of 0.1 to 1 m in normal conditions and up to 3 m in extreme conditions with high tidal velocities (> 1.5 m/s), as present at the Amazon shelf (Kineke et al. 1996). Marked interfaces (lutoclines) can be observed from echosounder recordings or from acoustic/nuclear density recordings. The flocs and particles in the fluid mud layer are supported by fluid drag forces exerted by the escaping fluid (hindered settling effect). The fluid mud layer can be subdivided into a turbulent upper layer (mixed fluid mud; 10 to 100 kg/m$^3$) and a laminar (viscous) lower layer (100 to 300 kg/m$^3$), depending on conditions. The turbulent upper fluid mud layer will try to (i) mix mud from the laminar lower layer into the upper turbulent layer and (ii) mix fluid from the upper dilute suspension layer into the fluid mud layer if the upper fluid mud layer is more turbulent than the dilute suspension layer (in accelerating spring tide flow). This results in a decreasing concentration in the upper fluid mud layer and a rise of the upper interface between the dilute layer and the fluid mud layer. If the dilute suspension layer is more turbulent than the fluid mud layer (in neap tide flow), the fluid mud layer will be relatively thin (much more stratified) and mud will be mixed up from the fluid mud layer into the dilute suspension layer by vortices from that layer. Stratified fluid mud near the bed is enhanced by salinity stratification during neap tide (damping of turbulence) at the frontal zone between river water and sea water. These processes are well described by Kineke et al. (1996) for the fluid mud system of the Amazon Shelf (South America). Transport of fluid mud will take place by tide-induced and wave-induced forces and gravity forces (sloping bottom).
- **Dilute mud suspension** with concentrations in the range of 0 to 10 kg/m³, which are detectable by optical methods and mechanical sampling (see Figure 2.1). Mud will be mixed into dilute suspension layer from the fluid mud layer if the the upper dilute layer is more turbulent than the fluid mud layer. Flocculation is dominant in the dilute suspension layer. The flocs and particles are supported by turbulence-induced fluid forces and transported by tide-driven and wind-driven currents.

Vertical layers of different densities are influenced by gravity processes which oppose the mixing processes. The stability of the system can be characterized by the gradient Richardson number (Ri) which includes the ratio of the concentration gradient and the velocity gradient. The concentration and velocity gradients are largest in the near-bed region. Larger mixing occurs for a larger velocity gradient. For Ri larger than about 0.2 (based on experimental data) with relatively large concentration gradients and relatively small velocity gradients, a stable system will be present (interfacial instabilities will die out and turbulence collapses).

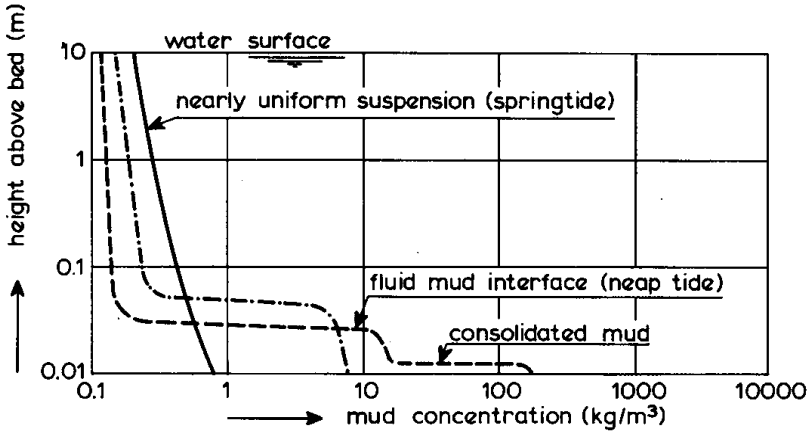


**Figure 2.1** *Schematization of mud concentration layers*

## 2.2 Fluid mud profiles of Amazon shelf, Ems river, Severn estuary, Wadden Sea channels

### 2.2.1 Amazon shelf

The Amazon shelf (Brasil) is the region extending from the shore to the shelf break at the 100 m depth contour. Much of the middle and inner shelf, landward of the 60-m depth contour, is characterized by a modern mud deposit (clays and silts) that appears to be a subaqueous delta prograding seaward over a transgressive sand layer. The middle shelf between about the 40- and 60-m depth contours has a relatively steep seaward gradient (> 1:500), and the broad smooth inner shelf (topset beds) has a gentle gradient (< 1:3000). There is a shore-perpendicular shoal (Cabo Norte Shoal) north of the river mouth and a transverse shoal (River Mouth Shoal) across the river mouth. The Amazon River discharge, the North Brazil current and the trade winds exhibit strong seasonal cycles . The mean Amazon River input of fresh water to the Atlantic is about 200,000 $m^3/s$, with a two-fold to three-fold difference between high discharge (May-July) and low discharge (October-December).
The Amazon surface plume of brackish water extends hundreds of kilometers seaward and northwestward along the coast. Much of the variability in surface salinity and currents can be accounted for by wind. The discharge of the Amazon is so large that seawater never enters the river mouth and many characteristic estuarine processes related to circulation and sediment transport occur on the Amazon shelf.

Mud concentration values at 2 stations (OS2 and CN) in the mouth of the Amazon river, Brasil have been reported by Vinzon and Mehta (2003). Both stations are located in the lee of Cabo Norte shoal and are sheltered from direct impact of the river runoff. The mean depth at the site is about 16 to 18 m. The spring tidal range is about 3.1 m. Due to the large river runoff, flow and sediment dynamics are dominated by estuarine processes up to a depth of about 100 m. A suspended sediment profiler was used to collect depth-profile data of the current by electromagnetic current meter and suspended sediment concentrations by optical backscatter instruments (OBS). The lowest measurement elevation was 0.25 m above the level at which the profiler rested on the bed.
**Figure 2.2** shows measured concentrations and flow velocities over the water depth at peak tidal flow; the data were composed from the measured data of Vinzon and Mehta (2003). The following features can be observed:

- lower fluid mud layer of about 2 m thick with high concentrations in the range of 10 to 200 $kg/m^3$; hindered settling is the dominant process (hindered settling layer); upward mixing by turbulence is almost nil as the turbulence is strongly damped; turbulence damping commencces for concentrations > 40 $kg/m^3$; the upper boundary of this layer is the lutocline (sharp almost horizontal interface with large concentration gradient); velocity profile is almost linear and is dominated by viscosity; majority of the sediment load is transported in this layer;
- well-mixed upper layer of small concentrations < 1 $kg/m^3$ (dilute suspension layer); settling velocities are relatively small in this layer; flocculation is minor; the suspended sediment is largely finegrained with a median (dispersed) grain size of about 3 $\mu$m; the mud concentrations in the upper layers are strongly dependent on the fresh water discharge coming from the Amazon river; at high discharges in May-June the mud concentrations in the entire upper layer up to the water surface increase to about 1 $kg/m^3$ (Kineke et al. 1996);
- intermediate mud suspension layer (flocculation layer) with concentrations between 1 and 10 $kg/m^3$; settling velocities are relatively large.

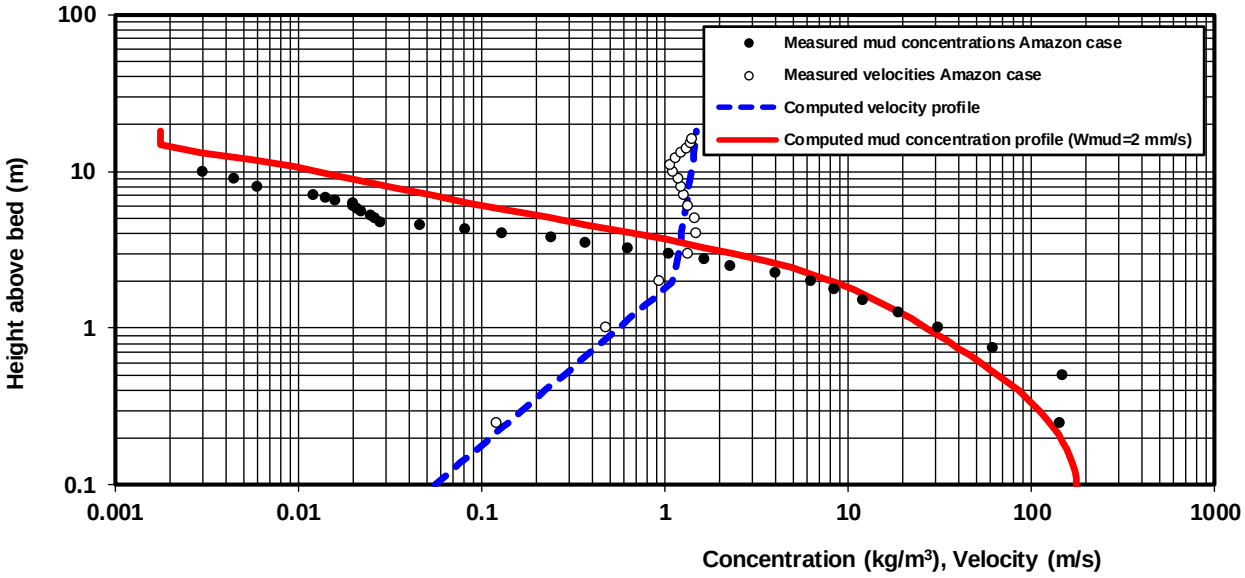


**Figure 2.2** *Measured and computed velocity, mud concentration and mud transport over the depth at peak flood flow for the Amazon mouth (Vinzon and Mehta 2003); computed values based on constant settling velocity of $w_{mud,max}$=0.002 m/s; damping coefficient $\alpha_d$= 1; $p_{mud}$=1*

Kineke et al. (1996) found three distinct vertical structures of fluid mud on the Amazon shelf:

- mixed fluid mud with vertically homogeneous concentration profiles and sediment concentration in the range 10 to 100 kg/m$^3$,with typically one lutocline at 10 kg/m$^3$, the elevation of which rose and fell in phase with the acceleration and deceleration of tidal currents; fairly high cross-shelf velocities within the fluid mud up to 0.5 m/s and velocities between 1 and 1.5 m/s in the upper layers;
- stratified fluid mud; stratified fluid mud is characterized by multiple lutoclines, with lutoclines at 10 kg/m$^3$ and at 100 kg/m$^3$; the high-concentration layer (> 100 kg/m$^3$) has a tickness of about 1 m; velocities between 1 and 1.5 m/s in the upper layers;
- high-concentration fluid mud; high-concentration fluid mud consisted of a thin layer (thickness of 1 m) of very high sediment concentration, on the order of 100 to 300 kg/m$^3$ with relatively low sediment concentration above it (< 1 kg/m$^3$); the velocities within this type of fluid mud were very low (<0.5 m/s).

### 2.2.2 Severn Estuary, UK

In the Severn, which is a vertically well-mixed macro-tidal estuary with a mean spring range of 12.3 m and a mean neap range of 6.5 m at Avonmouth, Kirby 1986 found that sediment begins to settle during the decelerating stages of the tidal cycles. As seen in **Figure 2.3**, lutoclines were observed to form relatively high in the water column at approximately 30% of the flow depth above the bed. As the flow continues to decrease towards slack, the lutoclines settle towards the bed, forming 2 to 3 m thick layers of fluid mud. After slack water during spring tides, the high-concentration fluid mud is normally re-entrained by the accelerating tidal currents. In the lower energy conditions prevalent during neap tides, the fluid mud that forms during decelerating tidal conditions is typically not completely re-entrained; instead, the lutoclines rise in the water column during accelerating currents and then resettle during decelerating currents. During intermediate tides, Kirby found that the lutoclines remain stable over several tidal cycles.
The dense mobile suspensions seem to be persistent through the neap-to-intermediate and intermediate-to-neap portions of the neap-spring cycle, and were observed to be advected up and down the estuary by

tidal currents without any appreciable vertical mixing. As the fluid mud movement slowed down during the stages of both flood and ebb tides, the fluid mud appeared to "move slowly over the bed partly or totally decoupled from the overlying water column." Thus, the fluid mud seemed to possess an inertia of its own, partially imparted by the drag from the overlying water and partially from gravity.

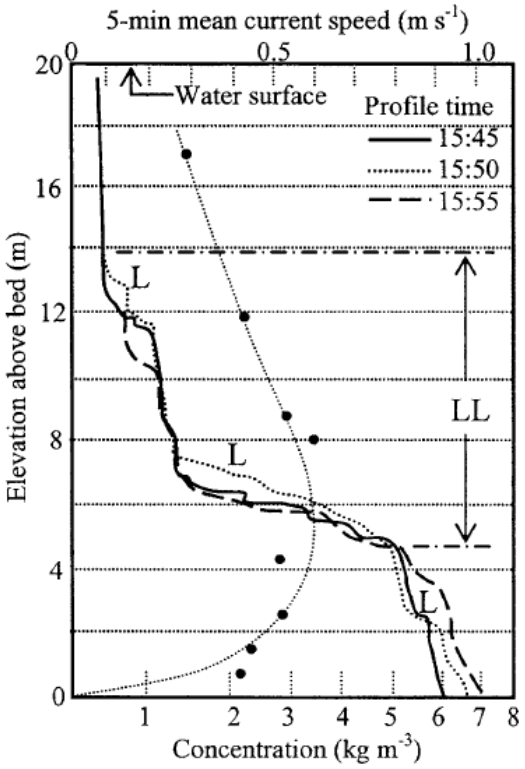


**Figure 2.3** *Mud concentration profile of Severn estuary, UK*

### 2.2.3 Tidal Ems river, Germany

The Ems-Dollard estuary, located on the border of the Netherlands and Germany, is forced by semi-diurnal tides with tidal ranges increasing from 2.3 m at the inlet to 3.5 m in the river (**Figure 2.4**). The system consist of the outer Dollard basin with intertidal flats (80% of total basin) and the tidal Ems river landward of Pogum (km 52). Channel depth is maintained at a navigable depth of 8 m from the barrier island of Borkum (km 0) to the harbor town of Emden (km 46) and at 7 m depth up to Papenburg (km 87). A tidal weir at Herbrum (km 100) marks the end of tidal system. The peak tidal velocities vary from about 1.5 m/s at Pogum to about 1 m/s at Papenburg. Freshwater discharges vary from 10 to 40 $m^3/s$ during the summer months to a maximum of 600 $m^3/s$ during wet winter periods (yearly average is about 100 $m^3/s$). The watershed of the Ems contains large areas of peat, which lead to highly refractory organic materials in the estuary. Information on the bed composition is given by Deltares (2014). Information on hydrodynamics is given by Van Maren et al. (2015).

In the period February 2005 to December 2007, 30 (nearly) monthly measurements of water quality, biological and sediment parameters have been done along the longitudinal axis of the Ems estuary (Talke et al. 2009). Profiles of velocity and backscatter concentration have also been collected with an ADCP and calibrated OBS-sensors.

Measurements show a wide variation range in suspended mud concentrations (SMC of 0.3 to 80 $kg/m^3$) during both ebb and flood tides (**Figures 2.5** and **2.6**). Water is relatively clear (SMC <0.5 $kg/m^3$) in the more marine portion of the estuary (salinity >10 psu) but is extremely turbid with large SMC and fluid mud (10 to

80 kg/m$^3$) in the brackish regions (salinity <2 psu). A high turbidity zone with a length scale of about 25 km is present between the toe of the salt wedge (km 65 to 75) to the tidal weir (km 100).

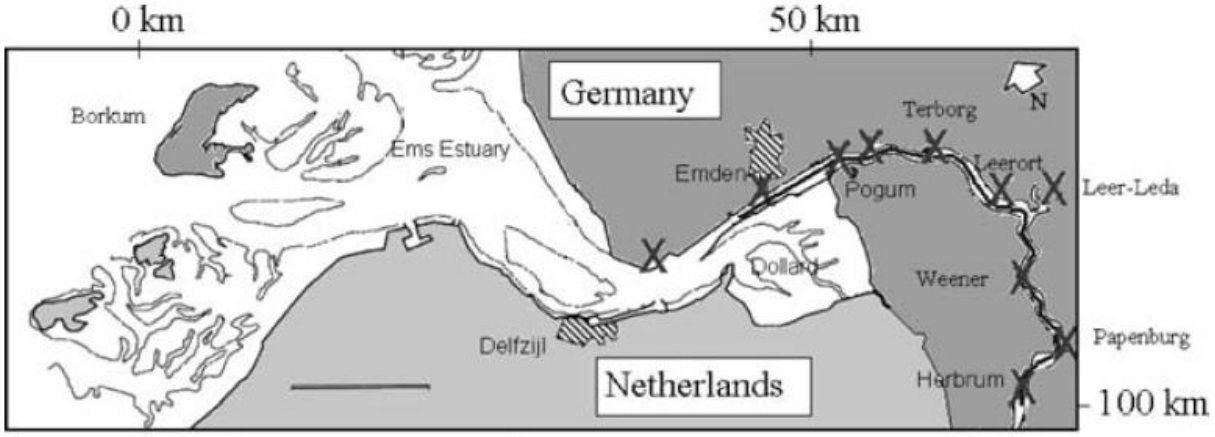


**Figure 2.4** *Planview of tidal Ems-Dollard system*

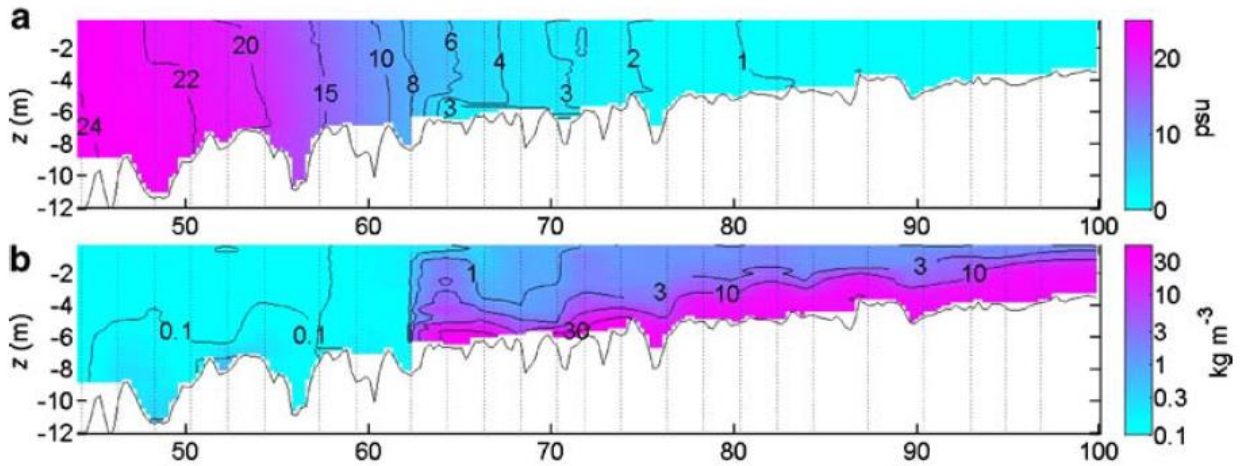


**Figure 2.5** *Salinity and suspended mud concentrations during ebb tide (2 August 2006) in Tidal Ems river*

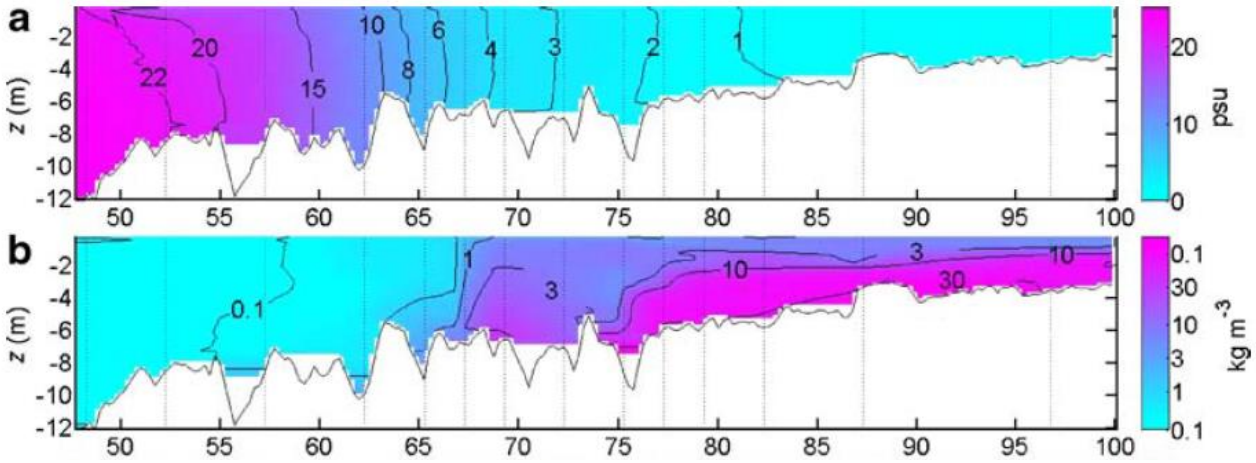


**Figure 2.6** *Salinity and suspended mud concentrations during flood tide (2 August 2006) in Tidal Ems river*

### 2.2.4 Tidal Holwerd Channel, The Netherlands

The tidal Holwerd channel is the fairway of the ferry between the village of Holwerd and the island of Ameland in the Dutch Wadden Sea, see **Figure 2.7**. The most eastward part of the fairway (length of 4 km, width of 50 m, depth of 4 to 4.5 m below mean sea level) near the ferry landing at Holwerd suffers from heavy siltation (dredging volume of about 2 million $m^3$/year). The tidal range is about 3 m; the local peak tidal velocities are in the range of 0.5 to 0.8 m/s during spring tide. The channel bed consists of muddy sand with $d_{50}$-values in the range of 63 to 125 μm; the channel bed at the corners and slopes of the cross-section consists of consolidated mud with dry bulk densities of 700 to 950 kg/$m^3$, see **Table 2.1**. The percentage of clay in the consolidated bed layer is about 15% to 20%.

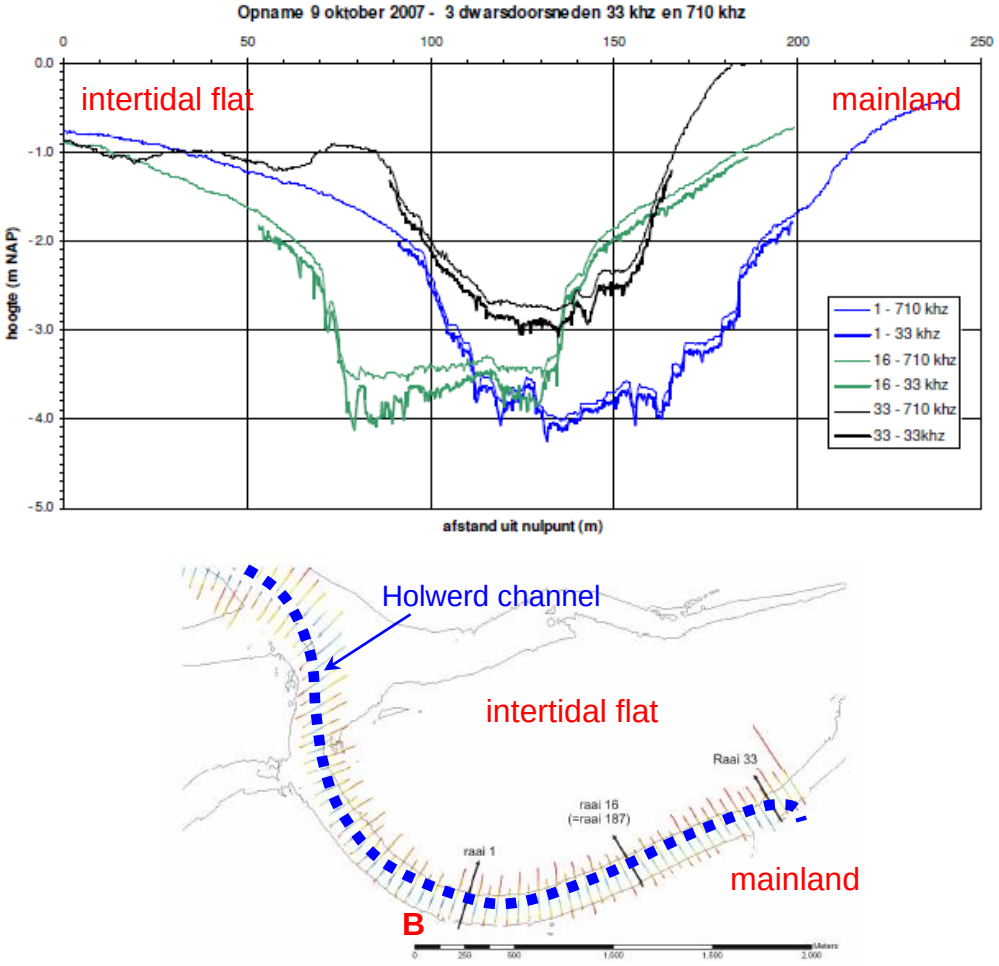


**Figuur 2.7** *Cross-sections 1, 16, 33; autumn 2007 (high- and lowfrequncy echosounding data)*

Field observations of suspended mud concentrations based on OBS-data show the presence of two distinct suspension layers at peak tidal flow (see **Figure 2.8**; Station B in **Figure 2.7**): a suspension mud layer of about 1 to 2 m with mud concentrations between 1 and 10 kg/$m^3$ and a dilute mud suspension layer of about 3 to 4 m with mud concentrationsn < 1 kg/$m^3$. Mud concentrations larger than 10 kg/$m^3$ have not been observed; the largest measured value is about 5 kg/$m^3$ (5000 mg/l). The mud concentrations decrease to about 150 mg/l during slack tide with low velocities of 0.1 to 0.2 m/s, see **Figure 2.8**.

Thin fluid mud layers with thickness < 0.3 m have been observed at various channel cross-sections during sounding surveys (33 and 210 kHz), see **Figure 2.7** (Deltares 2016b). Settling tests with mud concentrations between 10 and 50 g/l in a perspex tube show effective settling velocities in the range of 1 to 2 mm/s, see **Table 2.1**. This means that a fluid mud layer of 300 mm can settle in about 300 s and thus that the fluid mud will settle out rapidly during decelerating/slack tide. The relatively high bulk density of the consolidated mud bed also points to rapid settling of the high concentrations near the bed.

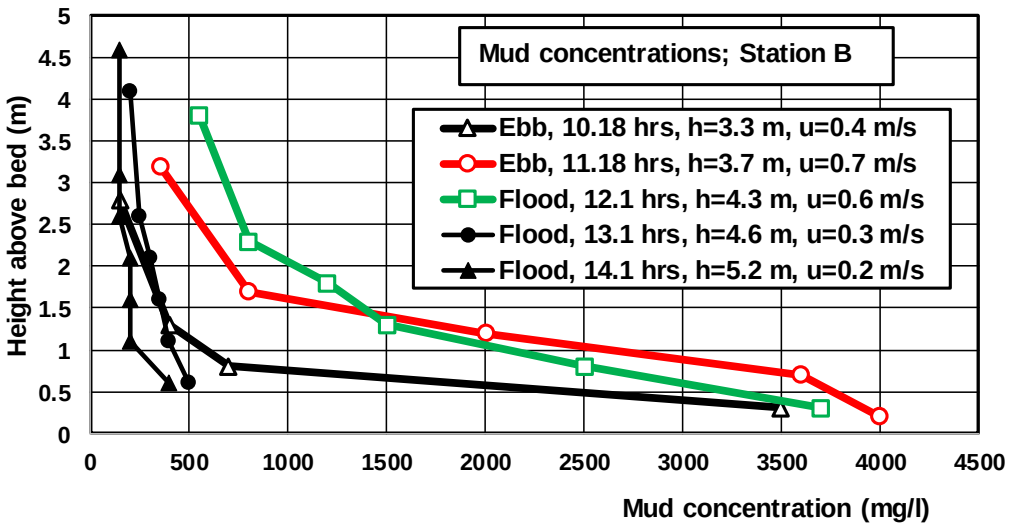


**Figure 2.8** *Mud concentrations (neap tide), Station B of Holwerd channel, Wadden Sea, The Netherlands*

| Field site | Hydrodynamic parameters | Suspension parameters | Effective settling velocity of fluid mud layer (mm/s) | Bed composition | | | |
|---|---|---|---|---|---|---|---|
| | | | | Percentage mud <63 μm and sand > 63 μm (%) | Percentage clay < 4 μm (%) | Dry bulk density (kg/m$^3$) | Gelling concentration (kg/m$^3$) |
| Amazon Shelf, Brasil | h≅ 15-20 m<br>H≅ 3-3.5 m<br>$U_{max}$≅ 1-1.5 m/s | FML≅ 2 m<br>SML≅ 2 m<br>DML≅ 10 m | ≅ 2 mm/s | muddy bed<br>$p_{mud}$> 80%<br>$p_{sand<}$ 20% | >30% | 200-300 | |
| Severn Estuary, UK | h≅ 5-20 m<br>H≅ 6-12 m<br>$U_{max}$≅ 1-1.5 m/s | FML< 1 m<br>SML≅ 6 m<br>DML≅ 15 m | | muddy sand in channel and mud at banks | >50% at banks | | |
| Tidal Ems River, Germany | h≅ 5-10 m<br>H≅ 3 m<br>$U_{max}$≅ 1-1.5 m/s | FML≅3-4 m<br>SML≅2-3 m<br>DML≅1-2 m | 1 mm/s at c=10 g/l<br>0.7 mm/s at c=60 g/l | silty-sandy mud at bed<br>$p_{mud}$≅70%<br>$p_{sand}$≅30%<br>$p_{org}$< 5% | 15%-30% | 200-300 | 200-250 |
| Wadden Sea, Holwerd channel, Holland | h≅ 4-5 m<br>H≅ 3 m<br>$U_{max}$≅ 0.5-0.8 m/s | FML<0.3 m<br>SML<2 m<br>DML≅ 4 m | 1-2.3 mm/s | silty-sandy mud at bed<br>$p_{mud}$≅60-80%<br>$p_{sand}$≅20=40%<br>$p_{org}$< 3% | 15%-20% | 700-950 | 100-200 |

h= water depth, H= tidal range, $U_{max}$= peak tidal velocity

FML= fluid mud layer with concentrations > 10 kg/m$^3$; SML=suspension mud layer with concentrations =1-10 kg/m$^3$, DML=dilute suspended mud layer with concentration < 1 kg/m$^3$

**Table 2.1** *Mud suspension parameters at various field sites*

### 2.2.5 General characteristics

The most basic fluid mud parameters (flud mud thickness, effective settling velocity, percentage of clay) of the former field sites are summarized in **Table 2.1**.
The maximum thickness of fluid mud layer is of the order of 2 to 3 m at the Amazon Shelf and in the tidal Ems river. The percentage of clay of the bed surface layer at these sites is larger than about 30%. The effective settling velocities of the fluid mud sediments are in the range of 1 to 2 mm/s. These relatively large values suggest that flocculation processes are dominant. The effective settling velocities of pure (primary) clay particles are much smaller (factor 10 to 100). Measured settling velocities of high-concentration clay suspensions (kaolinite clay < 2 μm; c = 10-100 kg/m$^3$) are of the order of 0.01 to 0.05 mm/s (Van Rijn 1993). The settling of a fluid mud layer with thickness of 1 m consisting of pure clay (< 2 to 4 μm) will take about 10 hours. Hence, a fluid mud layer with a relatively large percentage of clay cannot completely settle out during slack tide with low flow velocities.
The effective consolidation velocity of Bangkok fluid mud from c= 125 kg/m$^3$ to 250 kg/m$^3$ in a transparent perspex tube with initial height of 0.5 m takes about 1 week, which yields and effective settling velocity of 250 mm/(7x24x3600 s) ≅ 0.0005 mm/s (van Rijn 1993). Thus, the consolidation time scale of the top layer of the bed surface with concentrations > 125 kg/m$^3$ is of the order of weeks.

## 3. Fluid mud load predictions

### 3.1 Modelling of fluid mud

Two models are herein described: 1) 1D TMUD-model and 2) the 2DV SUSTIM-model

The TMUD-xls model is a quasi time-dependent model for simulation of suspended mud concentrations, load and transport in tidal conditions (Van Rijn 2016b). The model is most valid for saturated mud flow over a soft muddy bed in conditions where vertical transport processes are dominant (settling velocities > 0.5 mm/s) and horizontal gradients are relatively small. Mud loading due to horizontal gradients in flow velocity and tidal asymmetry are not included. The model is not valid for conditions with stagnant fluid mud due to horizontal trapping (navigation channels; harbour entrances).
The velocities and mud concentrations are computed as a function of z and t; z=height above bed and t=time (fixed time step of 5 to 15 min). The grid points over the depth (50 points) are distributed according to an exponential function. The settling velocity includes flocculation and hindered settling effects. Turbulence damping effects are taken into account by a damping function related to the local Richardson number (approach of Munk-Anderson 1948). Residual velocities due to salinity-indiced flow are taken into account if the salinity gradient and the fresh water river discharge are specified.
Measured mud concentration profiles at the time of maximum flow from the Amazon Shelf (dominant tidal processes) have been used for calibration of the model settings. Computed mud concentrations at the time of maximum flow are shown in **Figure 2.2** based on the following input parameters:
$p_{mud}$=1, $p_{sand}$=0, h= 17 m,
$\eta_{peak}$ = 1.5 m (Tidal range= 3 m), $H_s$= 0 m, $T_p$= 0 s,
$u_r$= 0 m/s (river velocity), $u_{c,peak}$= depth-averaged peak tidal velocity= 1.35 m/s,
T= 45000 s, $\varphi$=1 hours, $d\rho/dx$=0,
Settling velocities: $w_{mud,max}$= 0.002 m/s, $w_{mud,min}$= 0.0005 m/s,
Bed roughness values: $k'_{s,c,surface}$= 0.0001 m, $k_{s,c,velocity\ profile}$= 0.1 m, $k'_{s,w}$=0.0001 m,
$\rho_s$= 2650 kg/m$^3$, $\rho_w$= 1025 kg/m$^3$, $\nu$= 0.000001 m$^2$/s,
$\tau_{b,cr,mud}$= 0.1 N/m$^2$, a= 0.1 m, $\delta_{fm}$= 2 m, $\Delta$t= 900 s, $\alpha_{mud}$= 0.02, $\gamma_{mix}$= 0.3,
$\alpha_d$= 1 (Ri-approach for damping function), n=1.

The coefficient of the bed concentration function was fitted ($\alpha_{mud}$= 0.02) to obtain the best agreement of computed and measured values in the near-bed region. The settling velocity was represented by a constant value of $w_{mud,max}$= 0.002 m/s (2 mm/s).

The numerical SUSTIM-model solves the time dependent 3D advection-diffusion equation for suspended sediment concentrations (Van Rijn, 2023). The 3D advection-diffusion equation can be solved when the following parameters are known: 1) flow field (u, v, w); 2) sediment mixing coefficients ($\varepsilon_{s,x}$, $\varepsilon_{s,y}$, $\varepsilon_{s,z}$); 3) settling velocity ($w_s$) and 4) sediment concentrations at all boundaries and at initial time. The 2DV-model is derived from the 3D-model by setting the lateral components to zero.
The sediment mixing coefficients are related to basic current and wave parameters. The settling velocity depends on the sediment concentration to include the effects of flocculation and hindered settling in mud suspensions.
The bed-boundary condition (reference concentration) is represented by an empirical equation specifying the near-bed concentration as function of the local bed-shear stress.
The velocities and mud concentrations are computed as a function of z and t; z=height above bed and t=time . The grid points over the depth (25 to 100 points) are distributed according to an exponential function over the water column. The bed is defined at z=0. The grid points are distributed between z=0 and the water surface at each time. At least, 25 to 50 grid points are required for accurate results. The basic model processes and coefficients of both models (TMUD1D and SUSTIM2DV) are very similar.

### 3.2 Fluid mud thickness and mud load as function of velocity and water depth

The TMUD-model has been used to compute the depth-integrated mud load, the fluid mud layer thickness and the suspension layer thickness as function of the depth-averaged peak tidal velocity (between 0.5 and 2 m/s) and the water depth (5, 10 and 20 m), see **Figure 3.1**. The (mobile) fluid mud layer is defined as the layer with mud concentrations larger than 10 kg/m$^3$ at the time of maximum flow; near the bed the mud concentrations may be as large as 100 to 300 kg/m$^3$ (gelling concentration). This latter layer close to bed is herein called the super fluid mud layer. The maximum thickness of the super fluid mud layer can be estimated as the mud load divided by the gelling concentration. The suspension layer is defined as the layer with mud concentrations between 1 and 10 kg/m$^3$ at the time of maximum flow. The tidal range is set to 2 m. The phase shift between horizontal and vertical tide is set to 1 hour. The fresh water river discharge is zero. The horizontal salinity gradient is zero (seawater density= 1025 kg/m$^3$). The bed consists of mud (90%) and fine sand (10%). The critical bed-shear stress for erosion is set to 0.2 N/m$^2$. The settling velocity range is 0.1 to 1 mm/s; flocculation, hindered settling and turbulence damping are automatically taken into account. The erosion coefficient of the muddy bed is set to the default value $\alpha$= 0.003, which yields near-bed mud concentrations in the range of 0.5 to 50 kg/m$^3$ for velocities in the range of 0.5 to 2 m/s. The settings applied yield a relatively large thickness of the fluid mud layer. Similar computations for other settings yield smaller mud loads (factor 2).
The example computation results of **Figure 3.1** show that a mobile fluid mud layer ($c_{mud}$ > 10 kg/m$^3$) with a thickness of 2 to 3 m can be generated in a tidal channel with peak velocities between 1 and 2 m/s. The computed values of the fluid mud layer thickness are in good agreement with the observed values of 2 to 3 m at the Amazon Shelf (Vinzon and Metha 2003).
Mobile fluid mud can hardly be generated in a tidal channel for velocities < 1 m/s. Given a slack tide period of maximum 3 hours and a (low) effective settling velocity of about 0.1 mm/s for the fluid mud layer where hindered settling may be dominant, the maximum vertical settling distance is about 1 m. This means that a fluid mud layer with a thickness < 1m can largely settle out during slack tide of 2 hours. Fluid mud layers with thickness of 1 to 3 m generated by peak velocities between 1.5 and 2 m/s can only partly settle out during slack tide and will mostly be advected as mobile fluid mud up and down the tidal channel until the peak velocities reduce to less than about 1 m/s (during neap tide). Close to the bed a so-called super fluid

layer may be present. The maximum thickness of the super fluid mud layer is defined as the ratio of the depth-integrated mud load (see **Figure 3.1**) and the gelling concentration (assumed to be about 100 kg/m$^3$) resulting in values to up 1 m for conditions in which all mud particles are settled out (neap tide).
In a shallow tidal channel (depth< 5 m) with relatively low velocities between 0.6 and 0.8 m/s, a suspension layer of concentrations between 1 and 10 kg/m$^3$ and a thickness of the order of 1 m can be generated due to erosion of the local bed. The generation of a mobile fluid mud layer is hardly possible. Very thin fluid mud layers (< 0.3 m) may be formed locally during decelerating tide when settling processes are dominant.

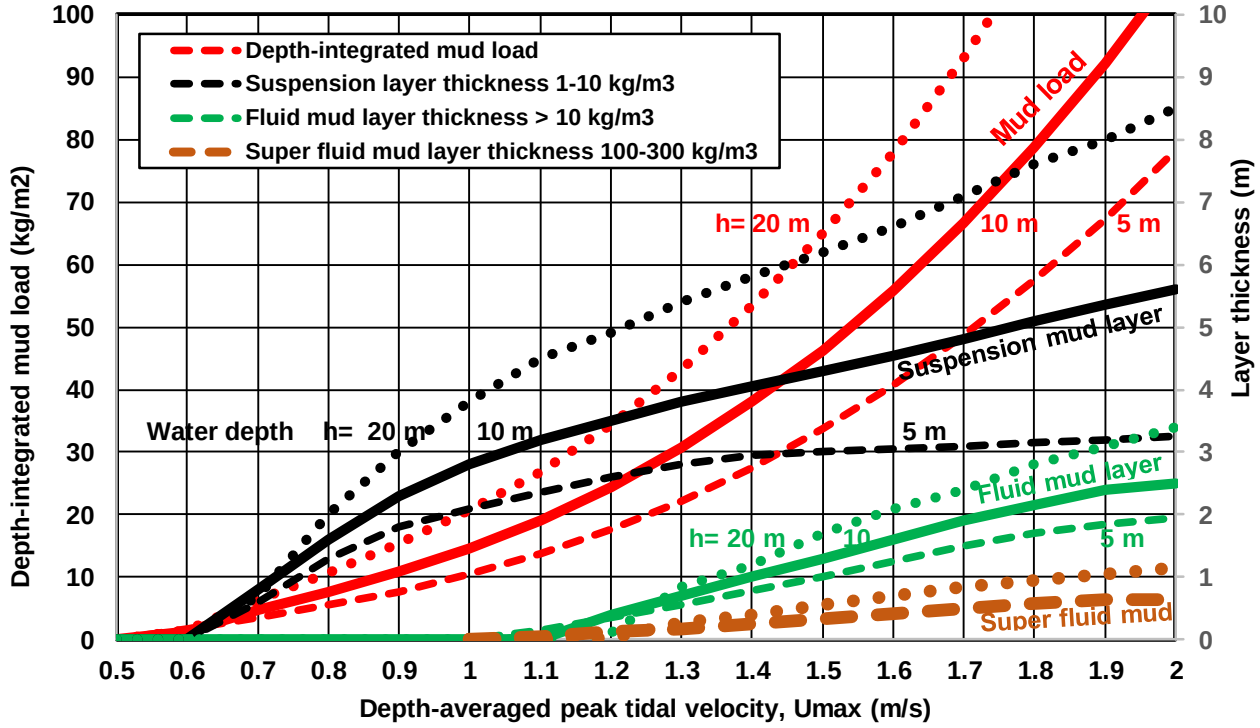


**Figure 3.1** *Mud load and mud layer thickness as function of peak tidal velocity and water depth (**red**= mud load; **black**= suspension layer 1-10 kg/m$^3$, **green**= fluid mud layer > 10 kg/m$^3$)*

**Figure 3.1** also shows that the depth-integrated mud load varies in the range of 10 to 100 kg/m$^2$ for velocities in the range of 1 to 2 m/s. Mud loads of 10 to 20 kg/m$^2$ correspond to the onset of fluid mud layer generation. Mud loads of 1 to 10 kg/m$^2$ can be generated in small-scale tidal channels with peak velocities in the range of 0.6 to 0.8 m/s.
**Figure 3.2** shows the effect of the significant wave height ($H_s$= 1 m and $T_p$= 7 s) on the mud load, suspension layer thickness and fluid mud layer thickness for a water depth of 10 m. The mud load increases by about 10 kg/m$^2$ for $H_s$= 1 m. The thickness of the mud suspension layer and the fluid mud layer increases significantly due to the presence of waves for current velocities below 1 to 1.2 m/s. At high current velocities the effect of waves is marginal, as the layer thickness is already relatively large.
Finally, it is noted that the TMUD-model is only valid for saturated mud flow over a soft muddy bed in conditions where vertical transport processes are dominant (settling velocities > 0.5 mm/s) generating mud concentrations increasing and decreasing over the tidal cycle; horizontal advection effects are not included. Therefore, the mobile fluid mud layer of both plots based on the TMUD-model may be somewhat too small (factor 2), as horizontal mud loading is manifest at most field sites and not represented by the TMUD-model. Both plots (**Figures 3.1, 3.2**) can be used to identify potential conditions for fluid mud formation.

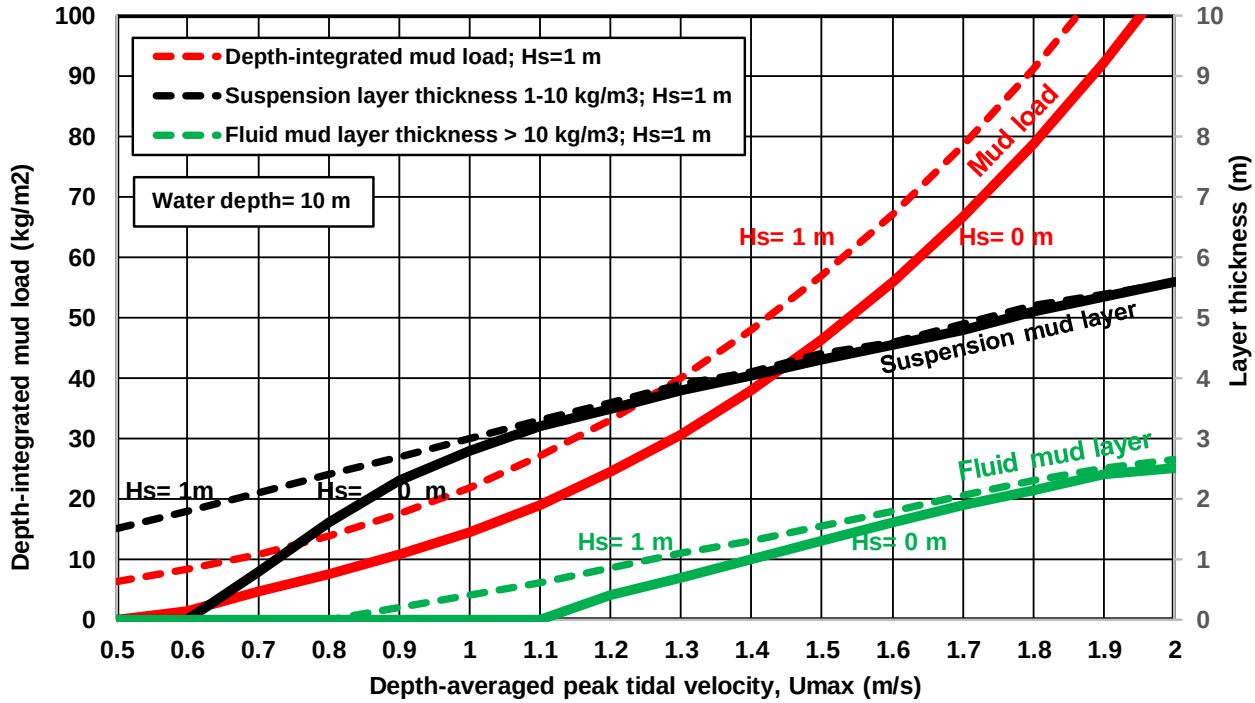


**Figure 3.2** *Mud load and fluid mud layer thickness as function of peak tidal velocity and wave height (**red**= mud load; **black**= suspension layer thickness, **green**= fluid mud layer thickness)*

### 3.3 Rapid infill of dredged shipping channel due to fluid mud

The SUSTIM2DV-model has been used to simulate the rapid infill of a dredged shipping channel due to the generation of fluid mud by currents and waves.
A trial dredge channel with length of about 1 km was made in the coastal waters of Bangladesh to study the deposition of fines in a local shipping channel. The local water depth is 8 m to MSL. The channel depth is 5.5 m below the surrounding bed. The bottom width of the channel is 100 m, see **Figure 3.3**. The tidal range is about 2 m. The local peak flood and ebb velocities are of the order of 1 m/s.
Many field surveys (13 hour measurements over the tidal cycle) were executed focusing on current velocities, mud concentrations, settling velocities and bed material sampling. In addition, various automatic recording instruments were deployed to measure currents, wave data and near-bed mud concentrations. Based on this, the local depth-mean mud concentrations were found to be in the range of 0.3 to 1.5 kg/m$^3$ during the monsoon period. The near-bed mud concentrations of exo-optical sensors at the bed were found to be in the range 1 to 10 kg/m$^3$. Most likely, the near-bed mud concentrations are higher (beyond the maximum saturation level of the sensors) in conditions with monsoon waves of about 2 m in a depth of 8 m.
The dredging works of the trial dredge channel with length of about 1 km were finished in September 2021. Bed level soundings showed very rapid infill of the trial channel within a period of 3 days (MBES-data and Admodus-bed density data), which was most likely caused by the generation of a fluid mud layer by the monsoon waves (in the range of 1 to 2 m in September 2021).
The basic input data are: water depth to MSL outside trench =8 m; tidal range= 2 m; approach angle=45°; depth-averaged current flood and ebb current=1 m/s; significant wave height=2 m; peak wave period =10 s; settling velocity mud=0.5 to 2 mm/s (variable); critical bed-shear stress for erosion=0.1 N/m$^2$; bed roughness=0.01 m; fluid density=1020 kg/m$^3$; dry bulk density= 800 kg/m$^3$; thickness fluid mud layer=0.5 m; mixing coefficients gam1=0.05, gam2=0.0025, gam3=0.25, gam4=0.25, n=2; turbulence damping parameter

alfad=1; NZ=50; time step=4 s.
The computed bed levels are shown in **Figure 3.3**. The test pit is almost completely filled with mud after 5 days due to the infill of fluid mud with concentrations in the range of 10 to 80 kg/m$^3$, see **Figure 3.3 (right)**. Only, the local generation of fluid mud can give such a rapid infill on a time scale of a few days.

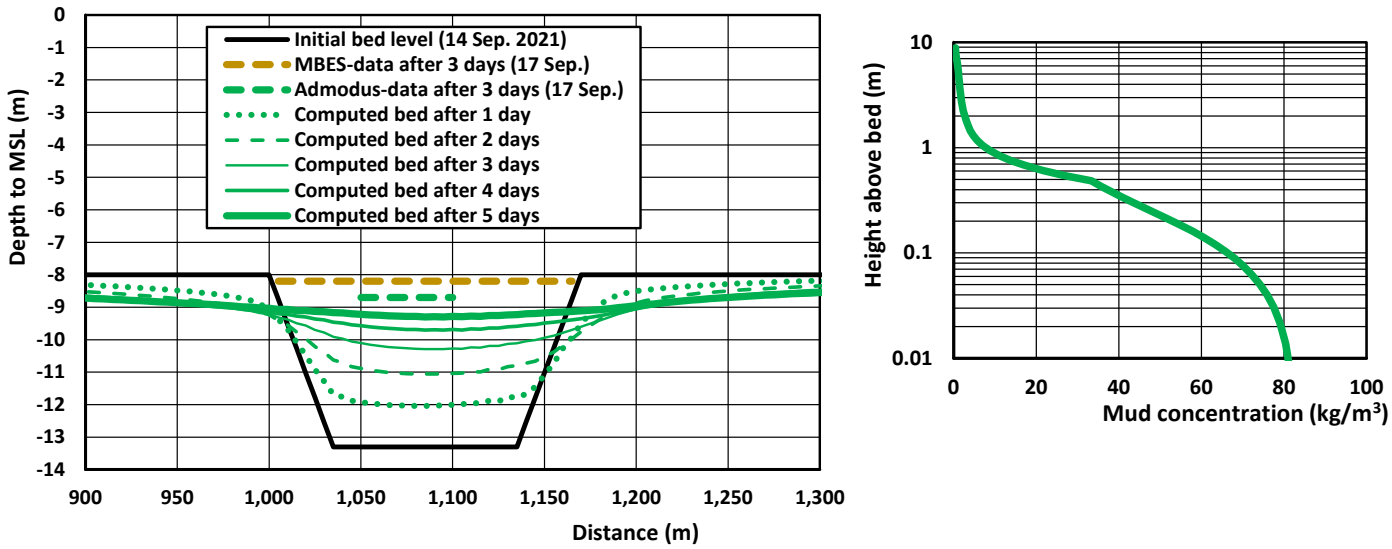


**Figure 3.3** *Measured and computed bed levels (left) and mud concentration profile at peak flow conditions outside channel (right), trial dredge channel Bangladesh*

## 4. Fluid mud formation and deposition

Fluid mud can form under various conditions:

***Supply/settling-dominated***

- settling of high-concentration mud suspensions *as stagnant fluid mud*; in low-flow areas in rivers, lakes, estuaries and coastal shelfs, thick fluid mud layers can be formed if the settling rates are larger than the dewatering rate of the bed surface (high percentages of clay);
- settling of mud suspensions *as stagnant fluid mud* in deepened navigation channels, mooring/turning basins, harbour basins; mud suspension becomes supersaturated due to the smaller bed-shear stresses and velocities; the vertical turbulence and concentration profiles decline, forming a fluid mud layer;
- supply of mud to and deposition *as stagnant fluid mud* at the landward end of converging and shallowing tidal channels by asymmetric tidal flows (high peak flood flows of short duration and low peak ebb flows of longer duration);
- high concentrations accumulating *as mobile fluid mud* near the edge of the salt wedge (turbidity maximum) in highly stratified estuaries; moving up and down the channel due to the tidal current;
- *mobile fluid mud*; gravity flows of a sediment-fluid mixture moving downslope under the action of gravity into a deeper navigation channel or filling low areas; three types of gravity flows are distinguished: a) flows supported in suspension by the turbulence generated by their own down-slope movement; b) non-turbulent fluid mud gravity flows; and c) gravity flows supported by the shear associated with ambient currents and waves;
- *mobile fluid mud*; fluid mud formations may be caused at open water dredged material disposal sites from where it is dispersed by currents and waves.

***Locally-generated***

- *mobile fluid mud*; erosion and settling of mud suspensions during accelerating/decelerating tidal flow (especially during neap tides); during slack water a temporary layer of fluid mud can be formed from the concentrations settling out from above; thickness of fluid mud layer will increase during neap tides;
- *mobile fluid mud*; fluidization by wave action; fluidization occurs when the soil matrix is destroyed by excess pore pressure buildup; the upwards pore water velocity exceeds the settling velocity of the grains; fluidization proceeds from the muddy bottom up, depending on the thickness of the muddy bottom and the degree of consolidation; soft sediment deposits can be easily fluidized by waves;
- *mobile fluid mud*; fluid mud generated by vessel-induced agitation of soft mud beds.

Locally-generated fluid mud can easily form in tidal flow with peak velocities of 1 to 1.5 m/s over a soft muddy bed. Sediments begin to settle during the decelerating stages of tidal cycles. As the flow continues to decrease towards slack, the lutoclines settle towards the bed, forming a thin layer of fluid mud. Dilute mud concentrations in tidal flow generally are in the range of 0.1 kg/m$^3$ (near the water surface) to 1 kg/m$^3$ (near the bed). The mud load, being the total amount of mud in the water column (of say 10 m), is in the range of $L_{mud}$= 1 to 10 kg/m$^2$. If this mud load is fully settled onto the bed as a fluid mud layer with density of $\rho_{dry}$= 100 kg/m$^3$, the thickness of the fluid mud layer is $\delta_{fluidmud} = L_{mud}/\rho_{dry}$ = 0.1 m.
After slack water during spring tides, the high-concentration fluid mud is normally re-entrained by the accelerating tidal currents. During lower energy conditions at neap tides, the fluid mud that forms during decelerating tidal conditions is typically not completely re-entrained; instead, the lutoclines rise in the water column during accelerating currents and then resettle during decelerating currents. Over longer time periods, the fluid mud consolidates to form a bed layer, which is called primary consolidation and associated dewatering.

# 5. Basic mud tests and properties

## 5.1 General

Mud properties of two types of mud samples should be determined:

- mud samples from bed surface layer using Van Veen grab, Ekman-grab, box-corer or drop corer;
- supended mud samples using bottle samples and/or pump samples.

Small subsamples of bed surface samples can be taken for determination of:

- percentage organic materials; percentage sand > 63 μm; percentage mud < 63 μm; percentage of clay < 4 μm;
- particle size distribution (PSD) of sand fraction > 63 μm (sieving method)
- particle size distribution (PSD) of mud fraction <63 μm using a) Laser-diffraction method, (Malvern Mastersizer), b) settling from uniform concentration suspension (Sedigraph method);
- settling velocity; settling tests from uniform suspension;
- dry and wet bulk density;
- undrained remoulded shear stress and flow point stress;
- critical bed-shear stress for erosion.

Suspended mud samples can be analyzed for determination of:

- particle size distribution (PSD);
- settling velocity of primary particles (laboratory); in-situ settling velocity is most important.

## 5.2 Mud particle size distribution (primary particles)

Sand and silt particles are almost spherical, but the fine sediment particles of the mud fraction have a flaky shape (plate-shaped) with an aspect ratio of $d_{mean}/\delta$ = 5 to 20 ($d_{mean}=0.5(d_{min}+d_{max})$, $\delta$=plate thickness, $d_{min}$=minimum diameter, $d_{max}$= maximum diameter, see **Figure 5.1.A**).

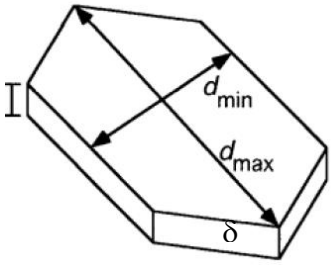


**Figure 5.1A** *Flaky plate-type clay/lutum particles*

Various methods are available to determine the particle size distribution of very fine sediments (clay, lutum), as follows:

- microscopic analyis method (Conley, 1965);
- settling column tests (hydrometer-test; pipet-test; SEDIGRAPH-test) yielding the equivalent (spherical settling) diameter based on the Sokes settling formula);
- Laser-Diffraction (LD) test yielding an equivalent diameter (Haverbeke 2013).

LD takes both the particle shape and its optic properties into account. The particle will scatter the incident light and through a number of detectors, the intensity and shape of this scattering pattern are measured. The Fraunhofer or the Mie theory can be used to interpret the obtained pattern. Larger particles will scatter strongly over small angles, small particles will do so more weakly and over greater angles.

Smaller particles will pass through the light source more than once (they are suspended in a closed water circuit). This should allow particles to pass with a different orientation each time, and thus let it define an 'equivalent spherical diameter'. That is, a sphere which would produce the same scattering pattern. The measuring range is 0.04 to 2000 µm.

The MALVERN Master Sizer (LD-instrument) is an attractive instrument to determine the particle size distribution (PSD) of the primary particles because the measurement is fast and simple using diluted samples. The MALVERN measures the volume of the particles which are converted to sphere-diameters. The laser beam passes through a dispersed particulate sample and the angular variation in intensity of the scattered light is measured. Large particles scatter light at small angles relative to the laser beam and small particles scatter light at large angles, see **Figure 5.1B**. The particle size is reported as a volume equivalent sphere diameter. The diffraction theory (Fraunhofer theory) is valid up to 10 times the wave length of the incident light, which means a lower limit of 7 to 8 µm. As the particles are circulated in suspension (by pump system), the particles pass the optical path many times at different orientations and so the shape effects are averaged out for spherical-type particles. Coarser and more angular sand particles are slightly overestimated (within 10%; Haverbeke 2013).
In the case of very small disc-type or plate-type clay partiles, it is not so clear what type of diameter is measured by the LD-method. Brown and Felton (1985) have found that the projected area of the plates (from which the LD-diameter $d_{LD}$ is derived) as seen by the LD is equal to 0.25 times the total area of the plates (two flat sides and two edge sides).
Thus: $0.25\ \pi d_{LD}^2 = 0.25[2x0.25\pi d_{plate}^2 + 2x\delta\pi d_{plate}]$ or
$d_{LD}^2 = d_{plate}^2\ [0.5 + 2(\delta/d_{plate})]$ or $d_{LD} = d_{plate}[0.5 + 2(\delta/d_{plate})]^{0.5}$ (4.1)
Assuming: $\delta/d_{plate} = 0.1$, it follows that: $d_{LD} \cong 0.85 d_{plate}$ or $d_{plate} = 1.2 d_{LD}$ (4.2)

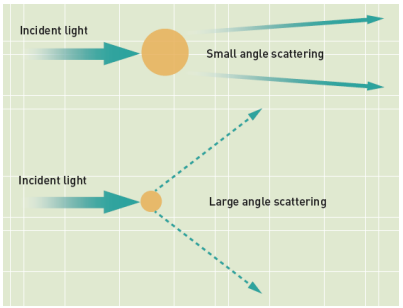


**Figure 5.1B** *Light scattering at small and large angles; Malvern method*

To determine the PSD of the primary particles, the diluted sample can be pre-treated with a chemical anti-flocculant and ultrasonic stirring, which will destroy all flocs. The sample concentration should be as uniform as possible, which is achieved by continuous recirculation of the sample volume (by pumping) during the measurement time. A sample dispersion unit is available for sample preparation.
It is remarked that due to extensive ultrasonic treatment, sand particles may break up, resulting in an overestimation of the finer fraction. Sensivity tests (Deltares 2014) show that ultrasonic treatment should not be longer than about 10 minutes.

The MALVERN (www.malvern.com) is known to underestimate the clay fraction (d < 2 µm). The fines are partly shadowed by the larger particles. This can be partly overcome by separating the finest fraction from the bulk by means of a settling test, in which the finest fraction remains in suspension after one hour. The ratio of the mass of the finest fraction to the overall bulk mixture can be calculated, and the PSD can be corrected with the psd of the finest fraction.

The SEDIGRAPH method (www.micromeritics.com) is based on X-ray absorption to determine the decrease of the sample sediment mass (concentration) as function of time from an initially uniform suspension.
The SEDIGRAPH uses a narrow beam of X-rays to measure directly the particle concentration in the liquid medium, see **Figure 5.2**. This is done by first measuring the intensity of a baseline or reference X-ray beam which is projected through the cell windows and through the liquid medium prior to the introduction of the sample. A homogeneously dispersed mixture of solid sample and liquid is next pumped through the cell. The attenuated X-ray beam is measured to establish a value for full scale attenuation. Agitation of the mixture is ceased and the dispersion is allowed to settle while X-ray intensity is monitored. During the sedimentation process, the largest particles fall below the measuring level, and progressively finer and finer particles do so until only the finest remain near the top of the measuring cell.
The sample container is about 100 ml; the initial concentration is about 100 to 1000 mg/l; ultrasonic stirring to obtain a uniform suspension can be (automatically) performed. The sand fraction > 63 μm generally is removed from each sample (by wet sieving). Organic materials and carbonates need to be removed from the sample with hydrogen peroxide and acid. Anti-flocculant can be used for optimum dispersion. Tests with and without anti-flocculants should be done. The settling velocity is converted to a PSD using Stokes' law. This conversion introduces an error, since Stokes' law is valid for spherical particles, whereas clays consist of plate-like particles which settle somewhat slower. Hence, the Sedigraph will underestimate the plate diameter in the clay/silt range and overestimate the clay fraction. The distribution of sediment with d > 63 μm can be determined by sieving, and subsequently added to the sedigraph-measurements to obtain the full PSD.

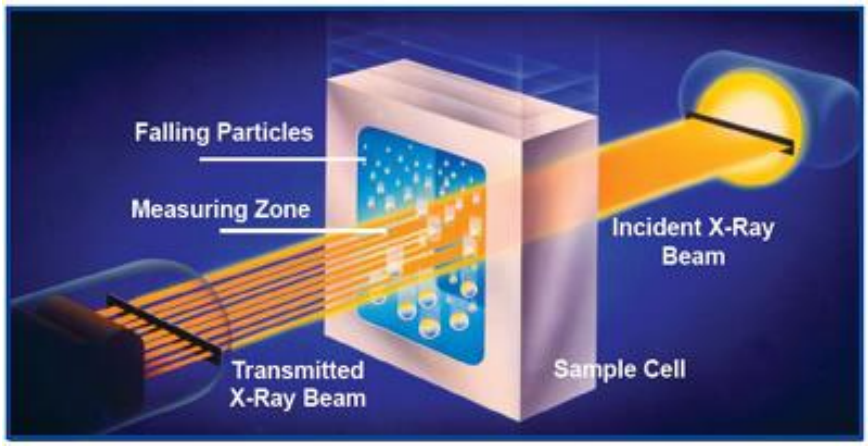


**Figure 5.2** *X-ray absorption of SEDIGRAPH instrument*

**Equivalent settling diameter, plate diameter and Laser-Diffraction (LD)-diameter**

The size of very small plate-type (disc-type) particles is most often derived as an equivalent spherical diameter based on the measured settling velocities from a settling test.
The equivalent spherical settling diameter $d_{sphere}$ follows from the Stokes settling formula, which reads as:
$w_s = (s-1)\, g\, (d_{sphere})^2/(18\, \nu)$
with: $w_s$= settling velocity, $s=\rho_s/\rho$= relative density, $\rho_s$= sediment density (2650 kg/m$^3$), $\rho_{s=}$= fluid density, $\nu$=kinematic viscosity coefficient, $d_{sphere}$= equivalent spherical settling diameter.

The settling velocity of a disc-type particle (thickness=$\delta$, plate or disc diameter= $d_{plate}$) falling with its flat side normal to the vertical direction can be derived from the drag force and the submerged volume weight.
The drag force is: $F_{drag} = 8\, \rho\, \nu\, d_{plate}\, w_s$ (www.Clarkson.edu) and the submerged volume weight is:
$G_{plate} = 0.25\, \pi\, d_{plate}^2\, \delta\, (\rho_s-\rho)g$.

The settling velocity is: $w_s = (s-1)g\,\delta\,d_{plate}/(32\nu)$

The settling velocity of a disc-type particle (thickness=$\delta$, diameter= $d_{plate}$) falling with its thin side normal to the vertical direction can be derived from the drag force and the submerged volume weight.
The drag force is: $F_{drag} = 5.3\,\rho\,\nu\,d_{plate}\,w_s$ (www.Clarkson.edu) and the submerged volume weight is:
$G_{plate} = 0.25\,\pi\,d_{plate}^2\,\delta\,(\rho_s-\rho)g$.
The settling velocity is: $w_s = (s-1)g\,\delta\,d_{plate}/(21.3\nu)$

Taken the settling of the disc and the sphere to be equal, it follows that:
- disc with flat side normal to vertical direction: $d_{plate} = 0.75\,(d_{plate}/\delta)^{0.5}\,d_{sphere} \cong 2.2\,d_{sphere}$ for $d_{plate}/\delta = 9$ (4.3)
- disc with thin side normal to vertical direction: $d_{plate} = 0.55\,(d_{plate}/\delta)^{0.5}\,d_{sphere} \cong 1.7\,d_{sphere}$ for $d_{plate}/\delta = 9$ (4.4)

If the settling velocity of very small plate-type clay particles is measured and converted to an equivalent spherical diameter using the Stokes settling velocity formula, the actual plate diameter of these particles is about 1.7 to 2.2 times larger than the equivalent spherical diameter (assuming $d_{plate}/\delta = 9$).

If the particle size is based on the Laser-Diffraction (LD) method, Equation (4.2) yields: $d_{plate} = 1.2 d_{LD}$
Based on Equations (4.3) and (4.4), $d_{plate} \cong 2\,d_{sphere}$ yielding $d_{sphere} \cong 0.6\,d_{LD}$.

Based on Equations (4.1), (4.3), (4.4), a general expression is: $d_{sphere}/d_{LD} = 1.1(d_{plate}/\delta)^{-0.25}$ (4.5)
Pabst and Berthold (2007) have given: $d_{50,sphere}/d_{50,LD} = 2.5(d_{plate}/\delta)^{-0.5}$ (4.6)
Both results are plotted in **Figure 5.3**.
Hence, the equivalent sphere diameters derived from settling velocity data are considerably finer (factor 1.5 to 2) than LD-diameters.

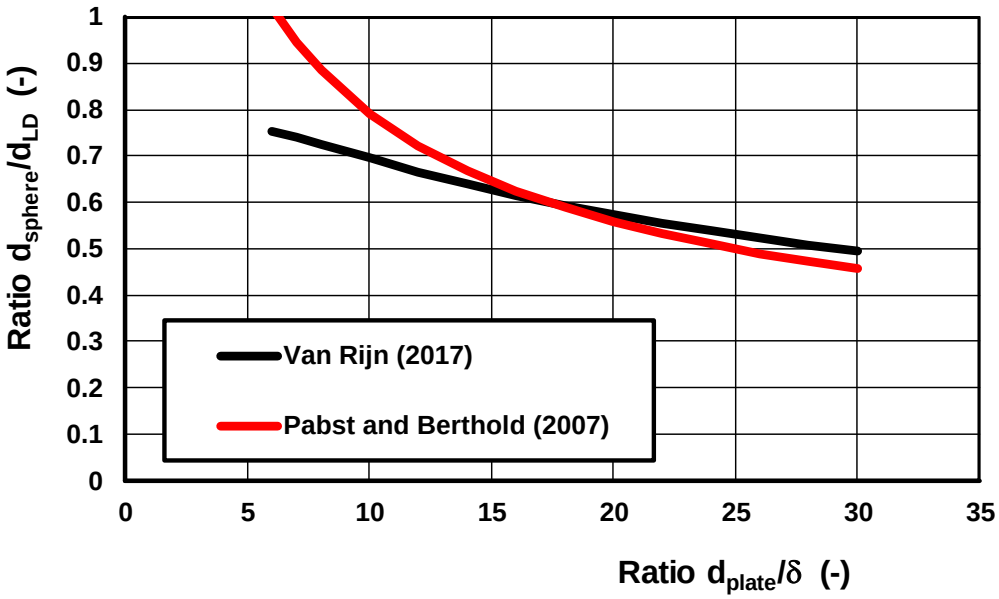


**Figure 5.3** *Ratio of sphere diameter and LD-diameter as function of $d_{plate}/\delta$*

**Comparison of particle size distributions of different analyis methods**

**Figure 5.4** shows the particle size distribution of Kaolin measured by the LD-method and by the hydrometer-method (based on measurement of fluid density decrease in a settling column), Haverbeke (2013). The $d_{50}$-value of the LD-method (≅7 μm) is much larger (more than factor of 2) than the equivalent diameter of the hydrometer-method (≅3 μm), which is caused by the particle shape effect of clay particles, see Equations (4.5) and (4.6).

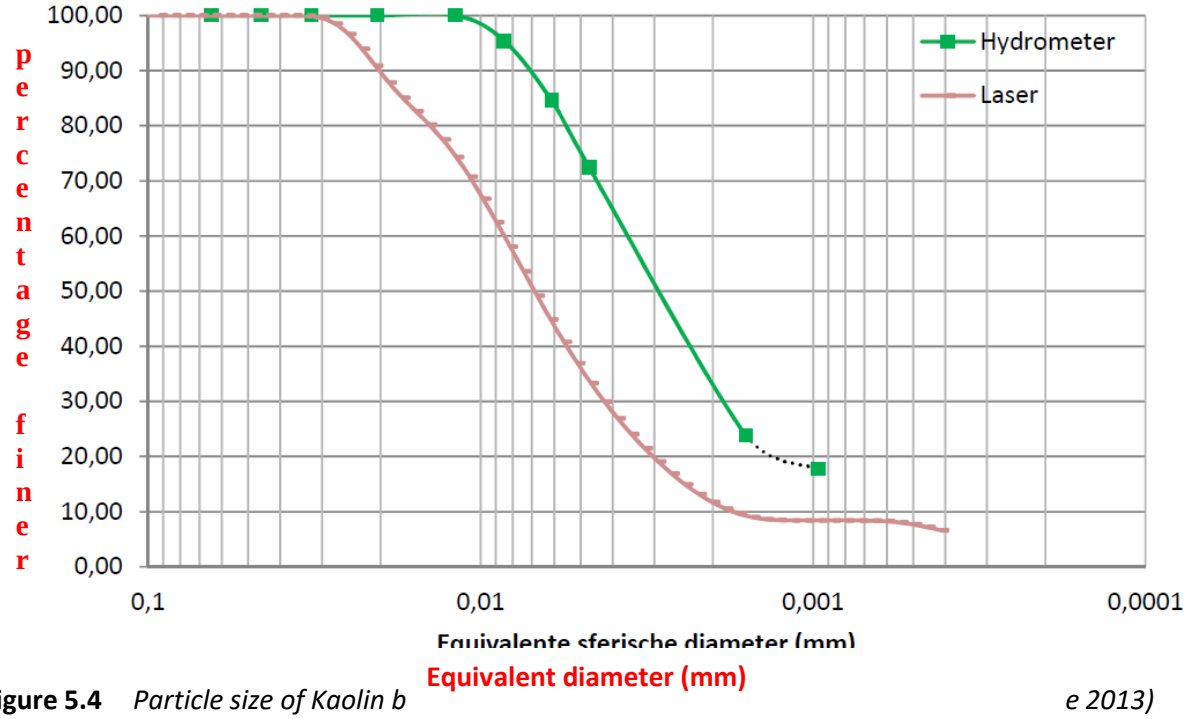


**Figure 5.4** *Particle size of Kaolin b* *e 2013)*

**Figure 5.5** shows particle size distributions measured using the SEDIGRAPH with and without chemical treatment (peptisator) for deflocculation. Based on this, the effect of chemical treatment is relatively small.
**Figure 5.6** shows particle size distributions (tidal channel, Noordpolderzijl, The Netherlands) of the complete mud-sand mixture, the mud fraction (SEDIGRAPH) and the sand fraction (sieving) separately.
**Table 5.1** shows particle sizes using the three methods for the same mud sample KG-14 (Holwerd channel, Wadden Sea).

| **Analysis method** | **Initial concentration; sample volume** | **$D_{10\%}$ (μm)** | **$D_{30\%}$ (μm)** | **$D_{50\%}$ (μm)** | **$D_{90\%}$ (μm)** |
|---|---|---|---|---|---|
| **MALVERN Laser-diffraction (1 test; mud+sand fractions without chemical dispersion)** | 100-1000 mg/l; ≅ 100 ml | 4 | 8 | 15 | 120 |
| **SEDIGRAPH method (1 test; only mud fraction < 63 μm with chemical dispersion)** | 100 -1000 mg/l; ≅ 100 ml | < 1 | 3 | 20 | 90 |
| **Sedimentation-Balance method (3 tests; mud+ sand fractions without chemical dispersion)** | ≅ 1000 mg/l ≅ 1000 ml | 20-30 (0.3-0.7 mm/s) | 35-45 (0.8-1.8 mm/s) | 45-95 (1.8-7 mm/s) | 115-300 (10-70 mm/s) |

**Table 5.1** *Particle sizes using three different methods; sample KG-14 (Holwerd channel, Wadden sea)*

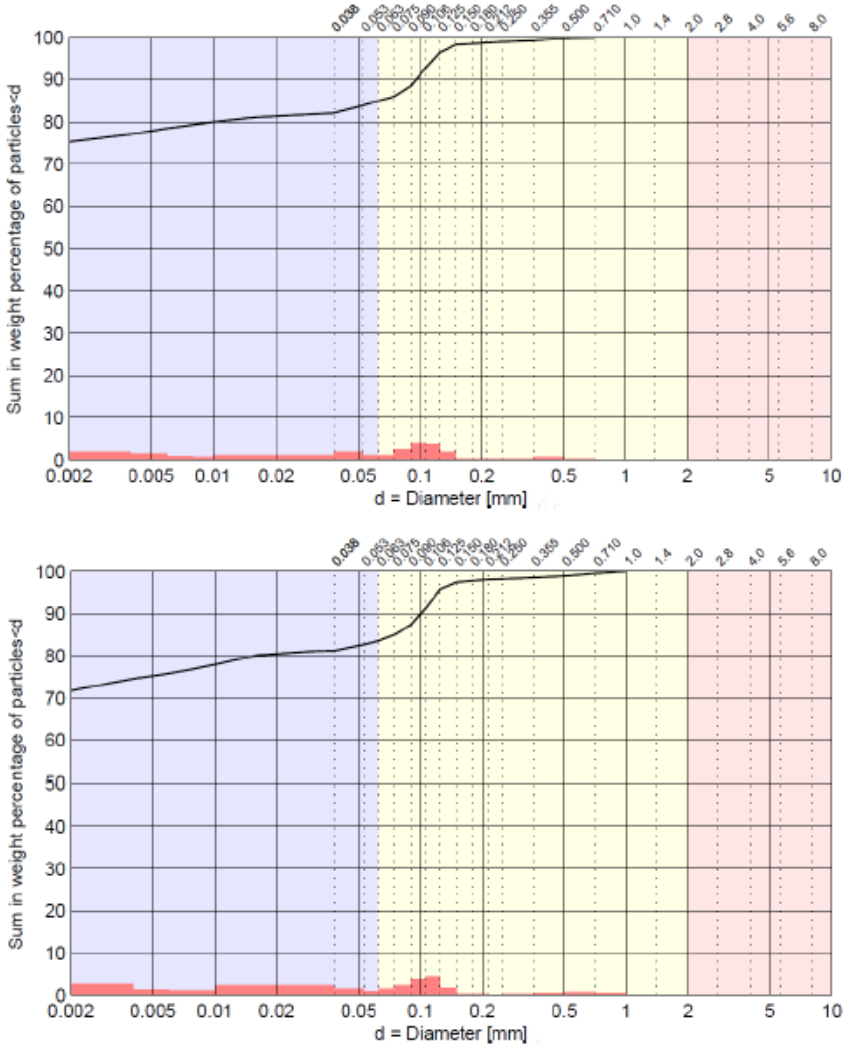


**Figure 5.5** *Particle size distribution of SEDIGRAPH with (upper) and without (lower) chemical treatment*

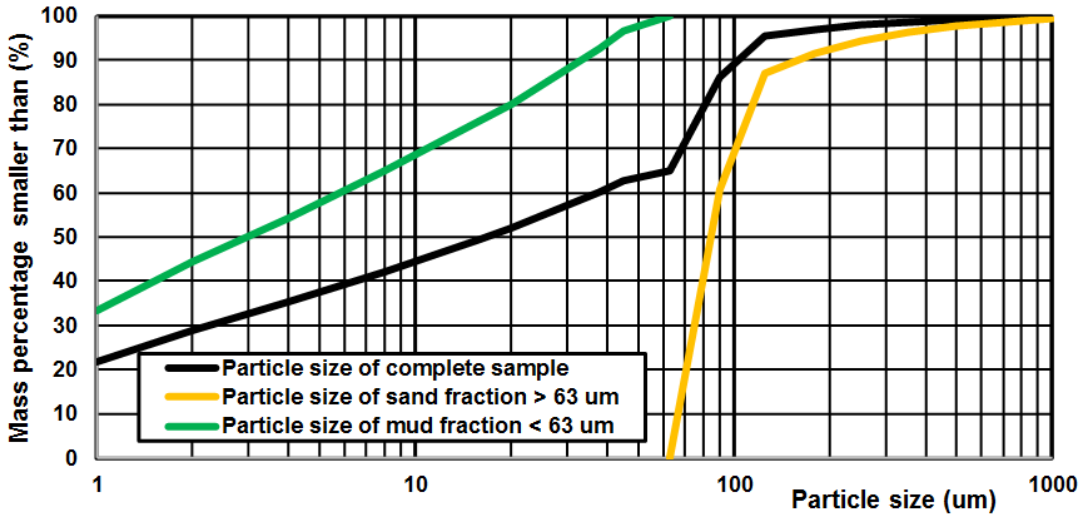


**Figure 5.6** *Particle size distributions of mud-sand mixture, mud fraction and sand fraction (tidal channel, Noordpolderzijl, The Netherlands*

**Figure 5.7** shows the particle size distribution of a bed sample from the Ems-Dollard tidal system based on the MALVERN method and the SEDIGRAPH method (Deltares 2014). The most striking difference is in the silt and clay range.
According to the SEDIGRAPH method, 20% of the sample is < 63 μm (mud) and 15% < 2 μm (clay).
According to the MALVERN, the clay content < 2 μm measured with the MALVERN is about 5%.

Based on the analysis of many samples, the MALVERN overestimates the mud content ($d$ < 63 μm), see **Figure 5.8**. Compared to the SEDIGRAPH results; the MALVERN strongly underestimates the clay content.

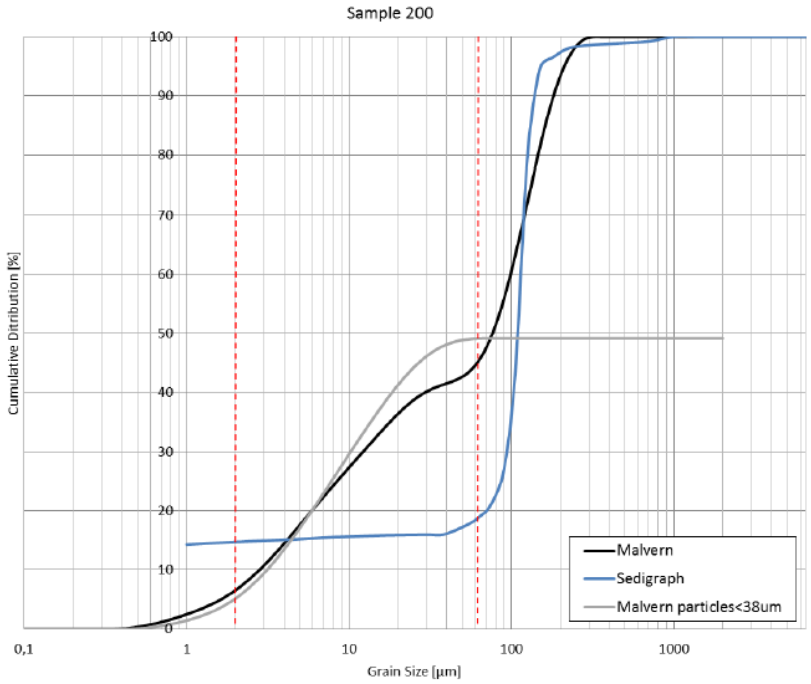


**Figure 5.7** *Particle size distribution of bed sample from Ems-Dollard tidal system using Malvern Laser-diffraction method and Sedigraph method*

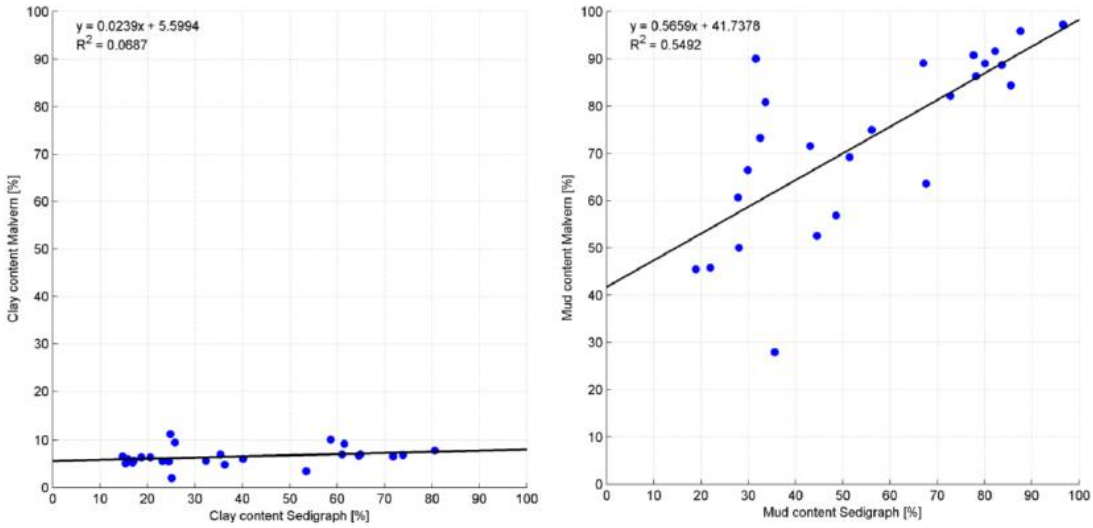


**Figure 5.8** *Clay content < 2 μm (left) and mud content < 63μm (right) based on Malvern and Sedigraph*

## 5.3 Effective settling velocity

### 5.3.1 Laboratory settling velocity at high concentrations (10-100 kg/m$^3$)

The effective settling velocity of the high-concentration fluid mud layer can be determined from laboratory settling tests in transparent perspex tubes/columns (with length of 0.6 m; diameter 0.1 m; volume of 3 liters; native water) using mud suspension in the range of 10 to 100 kg/m$^3$ (g/l), see **Figure 5.9**. Mud suspension of 10, 30 and 100 g/l can be made from the base mud samples taken from the bed surface (with dry bulk density of 200 to 400 g/l) by diluting using native, saline water.
At the beginning of the experiment, the sediment-water mixture is gently stirred (to prevent breaking of the flocs) to get a uniform distribution over the settling column. Over time, the sediments settle in the column and an interface between the water-sediment mixture and the clear water above becomes visible (hindered settling phase), see **Figure 5.9**. The end of hindered settling phase is characterized by the gelling concentration $c_{gel}$ at which a space-filling network develops, meaning that all particles are in contact with each other leaving no possibility for further settling. Consolidation starts immediately after this gelling concentration is achieved. After a while, the interface between clear water and the water-sediment mixture merges with the bed and the actual bed consolidation process starts, which is strongly related to the permeability of the soil. A camera can be used to take pictures of the column(s) at an increasing time interval, to be able to determine the position of the interface over time.
**Figure 5.10** shows the settling test results to estimate the effective settling velocity and gelling concentration for sample K-14 of Holwerd channel (Wadden Sea). The initial mud concentrations are 20, 40 and 60 g/l (kg/m$^3$). The gelling concentration can be roughly estimated from the mud height at the transition from settling to consolidation. The estimated gelling concentrations for KG-14 varies between 110 and 200 g/l. A rough estimate of the effective settling velocity can be estimated from the linear settling process (Phase I) of the test. This gives: settling velocity= settling height/time $\cong$ 340 mm/150 s $\cong$ 2.3 mm/s for an initial concentration of 10 g/l and about 0.25 mm/s for an intial concentration of 60 g/l. These values are in the range of the settling test results based on the Sedimentation-Balance method (see **Table 5.1**)

**Figure 5.9** *Settling tests using perspex tubes/columns*

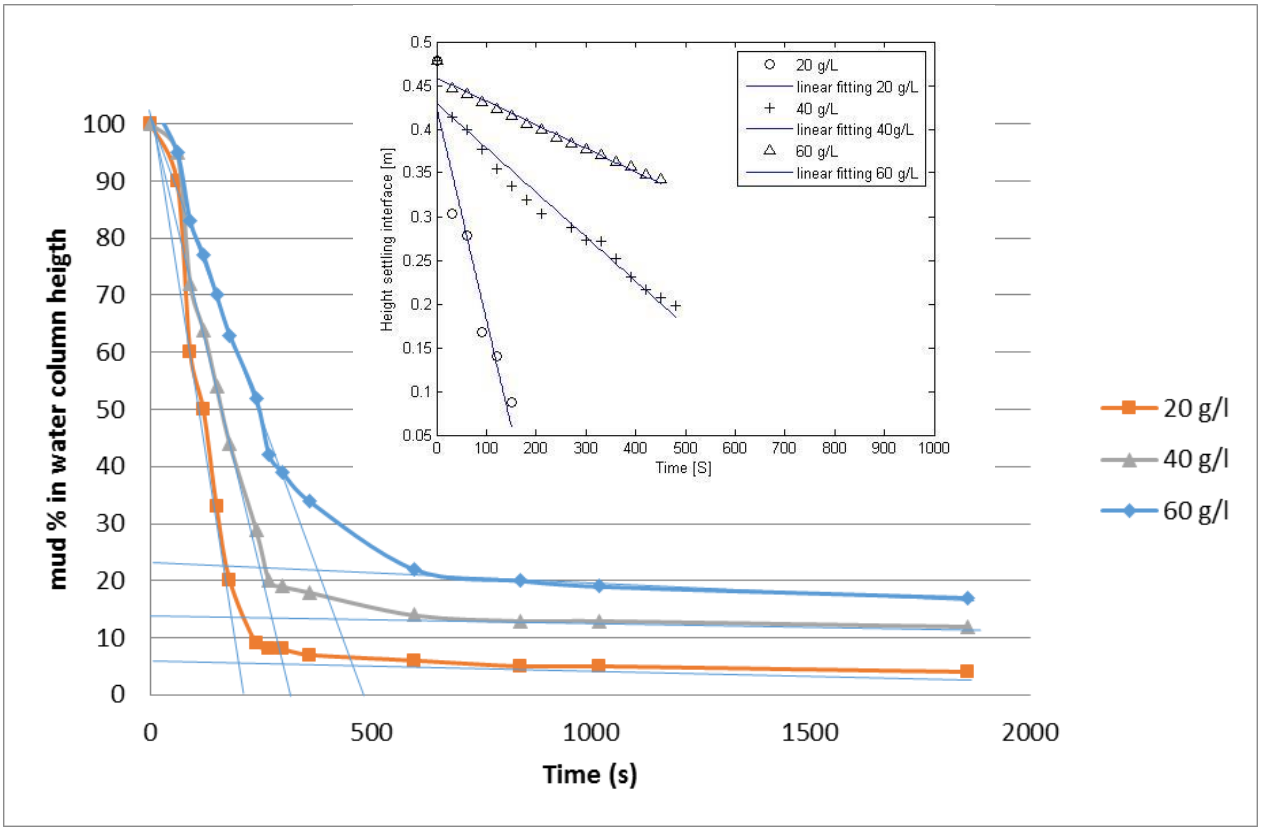


**Figure 5.10** *Settling test results of sample KG-14, Holwerd channel (Wadden Sea)*

### 5.3.2 Laboratory settling velocity at low concentrations (1 kg/m$^3$)

The Sedimentation-Balance method can be used to determine the settling velocity in the flocculation range of 0.1 to 1 kg/m$^3$, see **Figure 5.11**. The instrument consists of a temperature-regulated tube (double wall) with a height of 200 to 300 mm (about 0.5 to 1 litre) and an accurate weighing balance at the bottom of the tube. For reasons of accuraccy, the mud concentration in the settling column should be in the range of 100 to 1000 mg/l.

**Figure 5.11** *Sedimentation-Balance method of Deltares*

Two types of tests can be done:

- settling velocity of flocculated particles in suspension of native water;
- settling velocity of primary particles in suspension of fresh water with anti-flocculant (and initial ultrasonic stirring).

The sediment is dispersed in the tube by manual mixing to obtain a suspension with uniform concentration over the height of the settling tube; the balance bottom plate is connected to the electronic balance to weigh the accumulating sediment mass (under water) in time. The mass increase in time can be converted to settling velocity (known settling height) and to PSD using Stokes settling velocity formula.

Some results from the KG-14 sample (without anti-flocculant) are shown in **Table 5.1**. The particle sizes derived from the measured settling velocities are much larger than those from the Malvern-method and the Sedigraph-method. The latter two methods produce the size distribution of the primary dispersed particles, whereas the Sedimentation-Balance method produces the Stokes particles sizes of the sediments flocculating in the settling tube.

### 5.3.2 In-situ settling velocity

The in-situ settling velocity of suspended mud can be simply determined by using an in-situ settling tube. This method is based on the settling of suspended sediments from a uniform suspension in a small tube/ column (double walls in tropical conditions), see **Figure 5.12**.

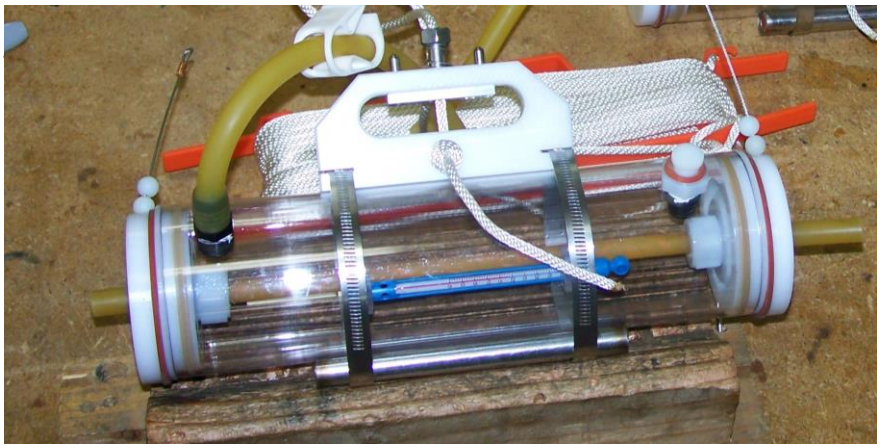

**Figure 5.12** *Sampling tube and settling column for in-situ settling velocity (WASED; www.wiertsema.nl)*

The sampling tube (length= 0.45 m, internal diameter= 0.1m, volume= 3.4 liters) is equipped with two valves on both ends. The tube is lowered from the survey boat to the sampling point in a horizontal position with opened valves. After closing the valves, the tube is raised. On board of the survey boat, the water-mud sample is poured into a separate settling column (length = 0.4 m; internal diameter= 0.1 m) with a closed bottom and a tap at 0.07 m above the bottom. The sample should be stirred carefully by a wooden stick with perforated bottom plate to create a homogeneous suspension after which the settling process starts (start of clock). Small subsamples of 50 ml are taken from the tap (0.07 m above the bottom) at pre-fixed times (t=0, 3, 6, 10, 20, 40, 60, 120 minutes). The basic principle of this method is to determine the decreasing sediment concentrations of an initially uniform suspension (dispersed system) at a pre-fixed point (depth) below the water surface as a function of settling time. Particles having a settling

velocity greater than the ratio of the depth and the elapsed time period will settle below the point of withdrawal after the elapsed time period. The precise analysis method is described by Van Rijn (2016).
**Figure 5.13** shows an example of measured settling velocities of flocculated and non-flocculated mud. The latter has been determined using the SEDIGRAPH III-instrument after mixing the sample with peptizer (for de-flocculation).

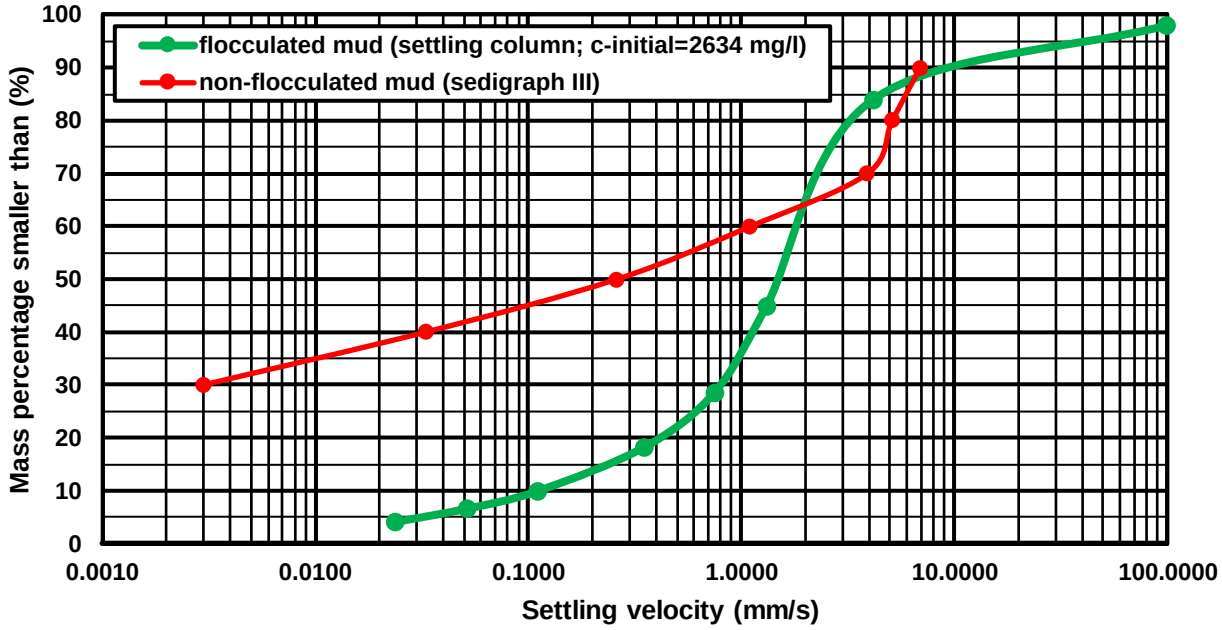


**Figure 5.13** *Settling velocities of flocculated and non-flocculated mud; Noordpolderzijl, Netherlands*

### 5.4 Dry and wet bulk density

Bed surface samples can be taken using mechanical grabs or corers operated from a survey vessel. Soft muddy beds can also be sampled by a diver pushing a plastic tube (length= 0.3 m, diameter = 0.05 m) into the soft bed. Preferably, the tube should be pushed vertically into the bed, but if the bed is too compacted the tube can also be pushed horizontally through the upper layer of the bed. The tube should be closed under water. The mass of the sample (M) can be simply weighed on board of the survey boat using a digital scale.
As the volume is known from the dimensions of the tube, the dry mass ($\rho_{dry}$) of the sediment volume can be determined from:

$\rho_{wet}$= M/V; $\rho_{dry}$= $M_s/V = \rho_s V_s/V$ and $\rho_{dry}=\{(\rho_{wet}-\rho_w)/(\rho_s-\rho_w)\}\rho_s$;

with: $M_s$= sediment mass in sample, $V_s$= volume of sediment= $(M-\rho_w V)/(\rho_s-\rho_w)$, V= volume of sample tube, M= mass of sample (water and sediment) $\rho_s$= sediment density (2650 kg/m$^3$), $\rho_w$ = fluid density of seawater (1020-1030 kg/m$^3$).

The water content is the ratio of the water mass and the sediment mass $=M_w/M_s=(V-V_s)/V_s$.
Some samples can be returned to the laboratory to determine: the percentages sand, silt and clay and the particle size distribution.

The in-situ wet/dry bulk density of the muddy bed surface can also be detected by using acoustic instruments (see **Figure 5.14**), consisting of acoustic transducers producing a series of acoustic waves. An envelop sound detector connected to a micro-processor is used to process the received signal, which is

compared to the signal in clear water. Calibration of the instrument is required. The linear dry density range is from 100 to 500 kg/m$^3$ (wet density of 1050 to 1300 kg/m$^3$) with an inaccuracy of ± 30 kg/m$^3$.

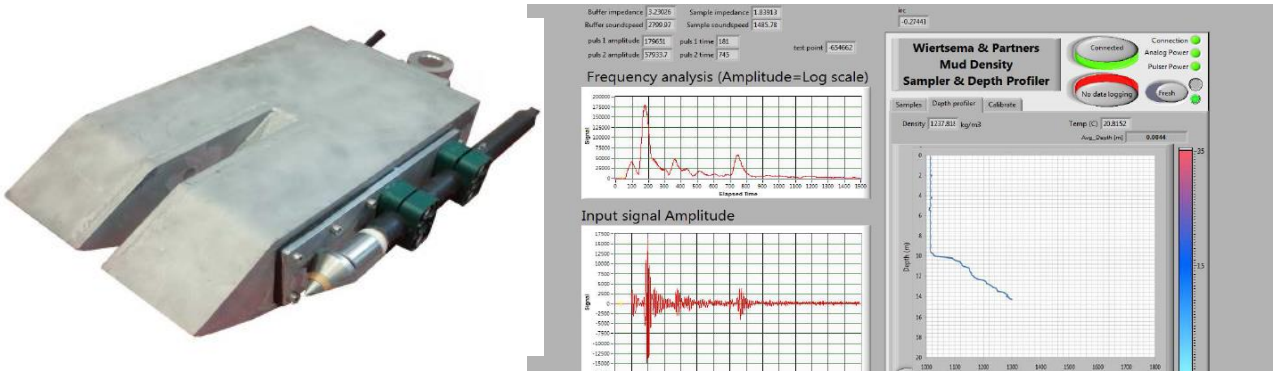


**Figure 5.14** *Acoustic profiler (Sonidense of Wiertsema.nl)*

## 5.5 Undrained (remolded) shear strength and flow point stress

The shear resistance of muddy soil is the result of friction and interlocking of particles, and possibly cementation or bonding at particle contacts. Due to interlocking, particulate material may expand or contract in volume as it is subject to shear-related deformation. If soil expands its volume (dilatation), the density of particles will decrease and the strength will decrease; and thus the peak strength would be followed by a reduction of shear stress. The stress-strain relationship levels off when the soil material stops expanding or contracting, and when interparticle bonds are broken. The theoretical state at which the shear stress and density remain constant while the shear strain increases may be called the critical state, steady state, or residual strength state. The residual strength is often termed as the remoulded shear strength.

If water cannot flow in or out of the pores of the particle skeleton, the shearing stresses are called the *undrained* stresses. During conditions with undrained shear, the density of the particles cannot change, but the water pressure and effective stress will change. On the other hand, if the fluid can freely drain out of the pores, then the pore pressures will remain constant resulting in *drained* shear stresses. The soil is free to dilate or contract during shear if the soil is drained. In reality, soil is partially drained, somewhere between the perfectly undrained and drained idealized conditions.

The undrained shear strength can be determined by a rotating vane test. The vane is pushed into the soil (in-situ or in the laboratory) and the vane is rotated at slow rate (5$^o$ to 10$^o$ degree per minute for a duration of 20 to 30 min). The torque is measured at regular time intervals. If the soil fails, the rotation rate will suddenly increase and the torque will decrease to a lower constant value which is used as an estimate of the undrained remoulded shear strength.

**Figure 5.15** shows the results of the shear strength measurements (Vane measurements) performed on various samples from the tidal Holwerd channel bed (Wadden Sea, The Netherlands). The peak shear strength is visible soon after the beginning of the test, with the remoulded strength being the strength at the end of the test.
The peak strength is a function of the rotation speed, stress history and the sample preparation. The undrained or remoulded shear strength is a material property at given water content of the sample and is

defined as the residual stress in the bed after failure of a sample. It gives an indication of the resistance of the sediment bed to mass erosion.

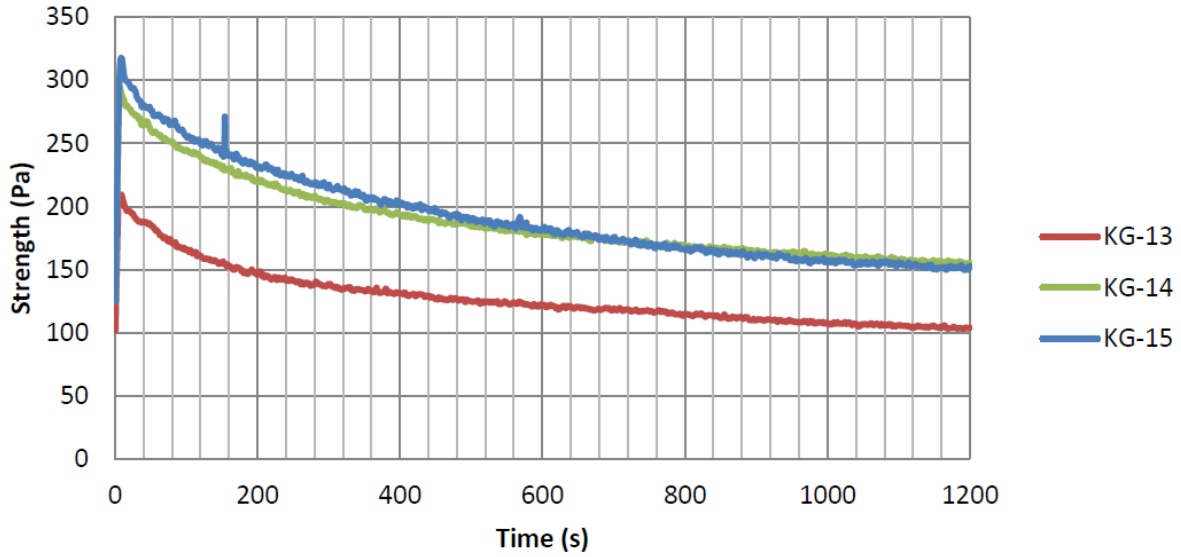


**Figure 5.15** *Shear strength (vane) measurements for samples KG-13, KG-14 and KG-15, Holwerd channel, Wadden sea (Deltares 2016a).*

The flow point stress of mud is the stress just before initiation of mud flow. It is the stress above which the mud sample behaves as a fluid, see **Figure 5.16**. At larger shear rates, the deformation rates are larger and more undrained conditions prevail (build-up of pore pressures). The flow point stress is a rheological parameter, which can be determined by tests in a roto-viscometer (plot of shear stress against shear rate).

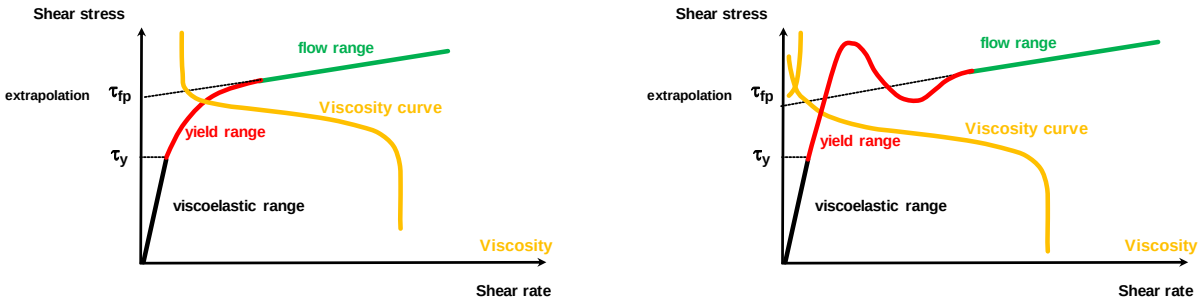


**Figure 5.16** *Shear stress as function of shear rate (du/dz)*

## 5.6 Critical bed-shear stress for erosion

The critical bed-shear stress for erosion can be determined by placing a mud sample in a laboratory flume, see **Figure 5.17**. The water discharge can be increased until particle/floc movement at the bedsurface is observed. The erosion rate of the mud surface just beyond initiation of erosion should not be larger than 1 mm per 15 minutes. The bed-shear stress can be derived from measured velocity profiles.

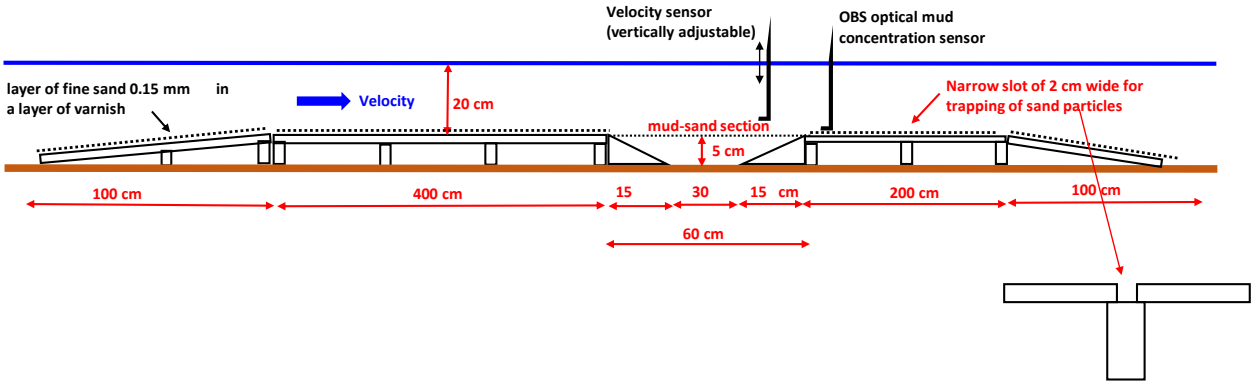


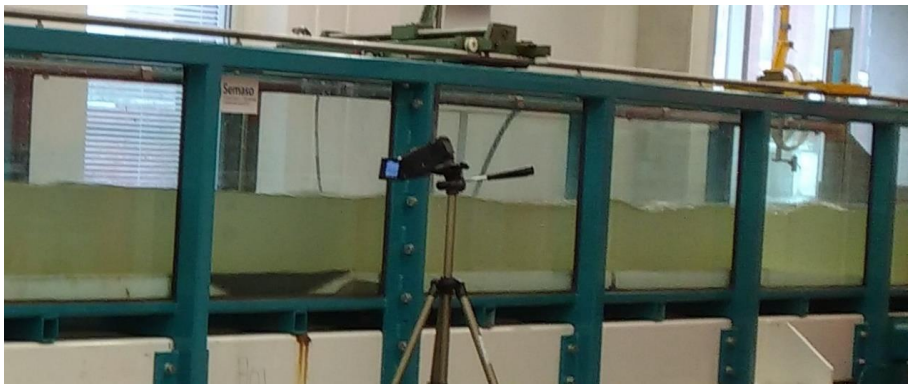

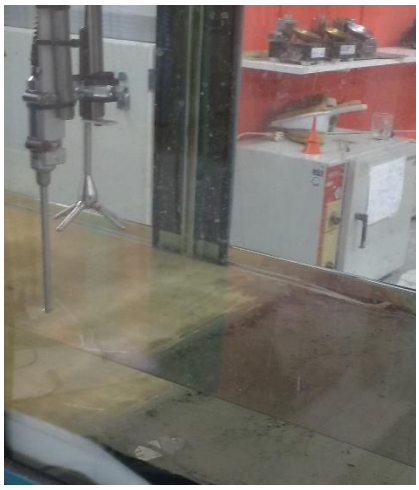

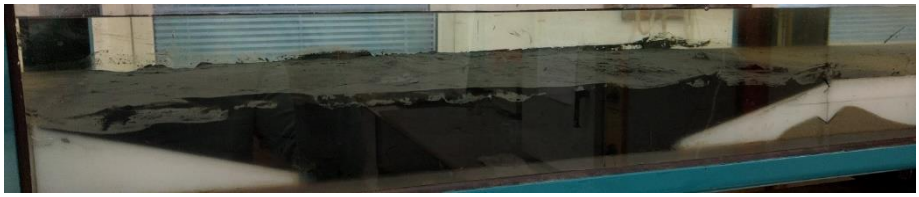

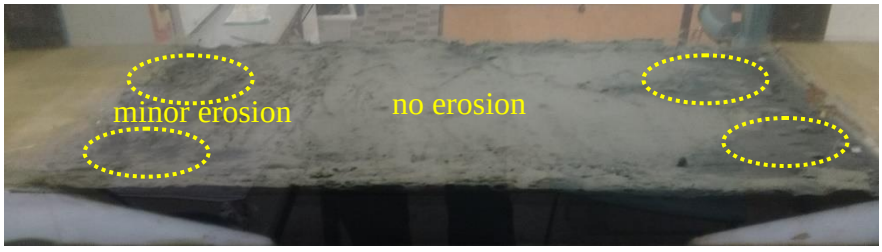


**Figure 5.17** *Flume setup for critical bed-shear stress of mud-sand beds*

A more simple method is the use of rotating propeller in a transparent tube (EROMES-instrument), see **Figure 5.18**. This latter method can also be used in-situ (Tolhurst et al., 2000; Van Rijn 2016a).

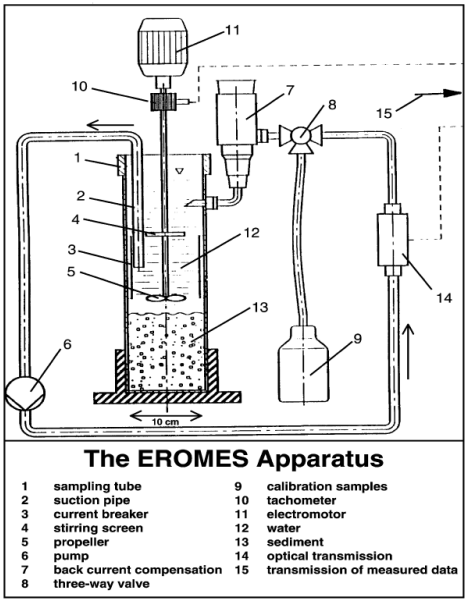


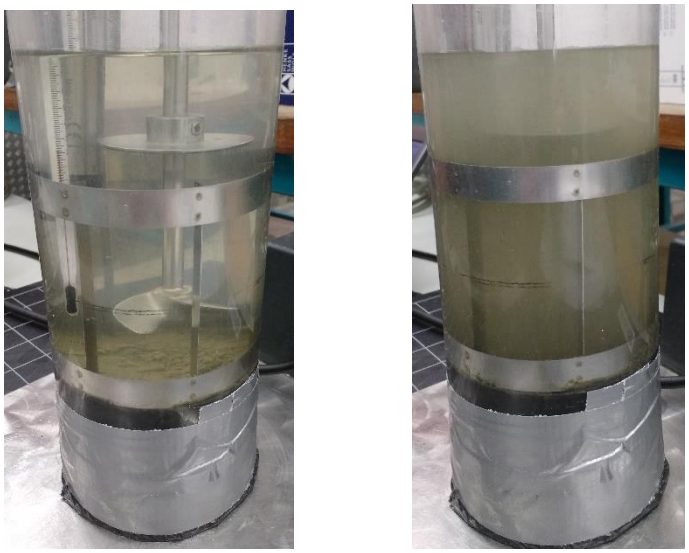

**Figure 5.18** *EROMES-apparatus*

Basically, the EROMES erosion instrument consists of a 100 mm diameter perspex tube that is pushed into the undisturbed bed sediment (in-situ or in the laboratory). The tube is gently filled with local (native) seawater and the eroding unit is placed on top of the tube. This eroding unit consists of a propeller (at fixed initial distance to bed surface of 30 mm) that generates a primarily tangential flow and associated bed-shear stresses. An optical OBS-sensor inside the tube monitors the changing suspended sediment/mud concentration. The propeller revolutions can be converted to bed shear stress by use of a calibration based on the onset of erosion of quartz sands with known critical erosion shear stress. During each erosion experiment, the bed shear stress is increased in steps of 0.1 N/m$^2$ every 2 minutes from 0.1 to 1 N/m$^2$ and the erosion rate can be determined after each step from the measured mud concentrations. The erosion thresholds can be determined by use of plots of erosion rates (in kg/m$^2$/s) versus applied bed stress.

## 6. References

**Brown D.J., Felton P.G.,** Direct measurement of concentration and size for particles of different shape using laser light diffraction, Chemical Engineering research and design 63 (2), 1985, 125-132
**Conley, R.F., 1965.** Statistical distribution patterns of particle size and shape in the Georgia Kaolins. Georgia Kaolin Research Laboratories. Elizabeth, New Yersey, USA.
**Deltares, 2014.** Mud dynamics in the Ems-Dollard, Phase 2: Analysis of soil samples. Report 1205711-001, Delft, The Netherlands
**Deltares, 2016a.** KPP Analysis tidal channel Holwerd-Ameland; Overview laboratory analyses. Report 1230378.002, Delft, The Netherlands
**Deltares, 2016b.** KPP Analysis tidal channel Holwerd-Ameland; Analysis of dredging data. Report 1230378.000, Delft, The Netherlands
**Haverbeke, J.P., 2013.** Comparison of Laser-diffraction method and Sieve-Hydrometer method for determination of particle size distribution of soil (in Dutch). Master Thesis, Department of Civil Engineering, University of Gent, Belgium
**Kineke, G. C., Sternberg, R. W., Trowbridge, J. H., and Geyer, W. R. 1996.** luid mud processes on the Amazon continental shelf. Continental Shelf Research, Vol. 16, 667–696.
**Kirby, R. 1986.** Suspended fine cohesive sediment in the Severn Estuary and inner Bristol Channel. Report No. ESTU-STP-4042, Dept. of Atomic Energy, Harwell, U.K., 242.
**McAnally, W.H. et al. 2007.** Management of fluid mud in estuaries, bays and lakes. Part I: Present state of understanding on character and behaviour. Journal of Hydraulic Engineering, Vol. 133, No. 1, 9-22
**McAnally, W.H. et al. 2007.** Management of fluid mud in estuaries, bays and lakes. Part II: Measurement, modeling and management. Journal of Hydraulic Engineering, Vol. 133, No. 1, 23-38
**Pabst W., and Berthold C.,** A Simple approximate formula for the aspect ratio of oblate particles, part. syst. charact. 24, 2007, 458-463
**Talke, S.A., De Swart, H.E. and De Jonge, V.N., 2009.** An idealized model and systematic process study of Oxygen depletion in highly turbid estuaries. Estuaries and coasts, Vol. 32, 602-620
**Tolhurst, T.J., Riethmueller, R. and Paterson, D.M., 2000.** In-situ versus laboratory analysis of sediment stability from intertidal mudflats. Continental Shelf Research, Vol. 20, 1317-1334
**Van Maren, D.S., Van Kessel, T., Cronin, K. and Sittoni, L., 2015.** The impact of channel deepening and dredging on estuarine sediment concentrations. Continental Shelf Research 95, 1-14
**Van Rijn, L.C. 1993**. Principles of sediment transport in rivers, estuaries and coastal seas. www.aquapublications.nl
**Van Rijn, L.C. 2016a**. Manual for sediment transport measurements. www.aquapublications.nl
**Van Rijn, L.C. 2016b.** Initiation of motion and suspension; critical bed-shear stress for sand-mud mixtures. www.leovanrijn-sediment.com
**Van Rijn, L.C., 2023.** Modelling of sand and mud transport in tidal flow; SUSTIM2DV-model. Report LVRS-Consultancy (www.leovanrijn-sediment.com)
**Vinzon, S.B. and Mehta, A.J., 2003.** Lutoclines in high concentration estuaries: some observations at the Mouth of the Amazon, p. 243-253. Journal of Coastal Research, Vol. 19, No. 2